Gondwana Research xxx (2009) xxx–xxx

Contents lists available at ScienceDirect

Gondwana Research

journal homepage: www.elsevier.com/locate/gr

Late Paleozoic volcanic record of the Eastern Junggar terrane, Xinjiang, Northwestern China: Major and trace element characteristics, Sr–Nd isotopic systematics and implications for tectonic evolution

Zhaochong Zhang [a,*], Gang Zhou [b], Timothy M. Kusky [c], Shenghao Yan [d], Bailin Chen [d], Li Zhao [a,c]

[a] State Key Laboratory of Geological Processes and Mineral Resources, China University of Geosciences, 29 Xueyuan Road, Beijing, 100083, China
[b] No. 4 Geological Party, Xinjiang Bureau of Geology and Mineral Resources, Altay, 836500, China
[c] Department of Earth and Atmospheric Sciences, 3642 Lindell Avenue, St. Louis, MO 63108, USA
[d] 26 Baiwanzhuang Road, Chinese Academy of Geological Sciences, Beijing 100037, China

ARTICLE INFO

Article history:
Received 11 October 2008
Received in revised form 7 March 2009
Accepted 7 March 2009
Available online xxxx

Keywords:
Volcanic rocks
Geochemistry
Island arc
Tectonic evolution
Junggar terrane
Northern Xinjiang

ABSTRACT

The Eastern Junggar terrane of the Central Asian Orogenic Belt includes a Late Paleozoic assemblage of volcanic rocks of mixed oceanic and arc affinity, located in a structurally complex belt between the Siberian plate, the Kazakhstan block, and the Tianshan Range. The early history of these rocks is not well constrained, but the Junggar terrane was part of a Cordilleran-style accreted arc assemblage by the Late Carboniferous. Late Paleozoic volcanic rocks of the northern part of the east Junggar terrane are divided, from base to top, into the Early Devonian Tuoranggekuduke Formation (Fm.), Middle Devonian Beitashan Fm., Middle Devonian Yundukala Fm., Late Devonian Jiangzierkuduke Fm., Early Carboniferous Nanmingshui Fm. and Late Carboniferous Batamayineishan Fm. We present major element, trace element and Sr–Nd isotopic analyses of 64 (ultra)mafic to intermediate volcanic rock samples of these formations. All Devonian volcanic rocks exhibit remarkably negative Nb, Ta and Ti anomalies on the primitive mantle-normalized trace element diagrams, and are enriched in more highly incompatible elements relative to moderately incompatible ones. Furthermore, they have subchondritic Nb/Ta ratios, and their Zr/Nb and Sm/Nd ratios resemble those of MORBs, characteristics of arc-related volcanic rocks. The Early Devonian Tuoranggekuduke Fm., Middle Devonian Beitashan Fm., and Middle Devonian Yundukala Fm. are characterized by tholeiitic and calc-alkaline affinities. In contrast, the Late Devonian Jiangzierkuduke Fm. contains a large amount of tuff and sandstone, and its volcanic rocks have dominantly calc-alkaline affinities. We therefore propose that the Jiangzierkuduke Fm. formed in a mature island arc setting, and other Devonian Fms. formed in an immature island arc setting. The basalts from the Nanmingshui Fm. have geochemical signatures between N-MORB and island arcs, indicating that they formed in a back-arc setting. In contrast, the volcanic rocks from the Batamayineishan Fm. display geochemical characteristics of continental intraplate volcanic rocks formed in an extensional setting after collision. Thus, we propose a model that involves a volcanic arc formed by northward subduction of the ancient Junggar ocean and amalgamation of different terranes during the Late Paleozoic to interpret the formation of the Late Paleozoic volcanic rocks in the Eastern Junggar terrane, and the Altai and Junggar terranes fully amalgamated into a Cordilleran-type orogen during the end of Early Carboniferous to the Middle–Late Carboniferous.

1. Introduction

The Central Asian Orogenic Belt (CAOB), one of the largest accretionary orogenic belts in the world, formed largely by subduction and accretion of juvenile material during the Neoproterozoic and Paleozoic (Sengör et al., 1993; Windley et al., 2002; Xiao et al., 2003, 2004, 2008; Jahn, 2004; Kovalenko et al., 2004; Kuzmichev et al., 2005; Safonova et al., 2002; Zhai et al., 2007; Chai et al., 2009-this issue; Zhao et al., 2009-this issue). Since the 1990s, the CAOB has received more attention because it is very important not only for understanding the tectonic evolution and amalgamation history of Central Asia, but also for understanding the processes of continental crustal accretion and metallogenesis. Some models have been proposed to explain the development of the CAOB. Mossakovsky et al. (1994) suggested the closure of small ocean basins by multiple subduction, the obduction of ophiolites and the accretion and collision of island arcs and microcontinents, whereas Sengör and his colleagues envisaged continuous lateral accretion along the southern margin of the Siberian plate along a single subduction zone (Sengör et al., 1993; Sengör and Natal'in, 1996; 2004). More recent investigations have revealed, however, that the CAOB contains various terranes indicating

* Corresponding author. Tel.: +86 10 82322195.
E-mail address: zczhang@cugb.edu.cn (Z. Zhang).

1342-937X/$ – see front matter © 2009 International Association for Gondwana Research. Published by Elsevier B.V. All rights reserved.
doi:10.1016/j.gr.2009.03.004

a more complex tectonic history (Lamb and Badarch, 2000; Heubeck, 2001;Windley et al., 2002; Khain et al., 2003; Xiao et al., 2003, 2004, 2008; de Jong et al., 2006, Cocks and Torsvik, 2007; Kröner et al., 2007). For a better understanding of the history of the CAOB, these models need to be re-tested and augmented with new geochemical data.

The Junggar terrane is situated in the central part of the CAOB (Fig. 1a), and Devonian to Permian volcanic rocks are well exposed in the terrane. Hence, it offers an excellent opportunity to understand the tectonic evolution during the Late Paleozoic. In this paper, we present new geochemical data for the Late Paleozoic volcanic rocks from the Eastern Junggar terrane and use these data to constrain their genesis and tectonic setting. These data also provide new constraints on geodynamic models for the tectonic evolution of the Eastern Junggar terrane.

2. Geological setting

The Junggar terrane is located between the Siberian plate, the Kazakhstan block, and the Tianshan Range (Fig. 1b). They are part of the great CAOB, which extends from the Uralides in the west to Sikhote–Alin'in, where it is truncated by Pacific subduction–accretion systems of Mesozoic age, and are bounded to the north by the Siberian craton and to the south by the Tarim cratonic block. The >2500 km long and up to 50 km wide Irtysh fault, which is generally considered to be the north boundary of the Junggar terrane, is interpreted as either a strike-slip fault accommodating >1000 km of syn-subduction strike-slip motion (Sengör and Natal'in, 1996) or a suture between the Altai arc, which rims the Siberian craton, to the north and the Junggar microcontinental block to the south (Coleman, 1989; and references in Briggs et al., 2007). In both models, the Irtysh fault figures prominently, either as a roof fault of a large strike-slip duplex system developed during oceanic subduction or as a suture of arc–continent or continent–continent collision. These models suggest significant Permian shortening and exhumation during motion on the Irtysh fault after ocean closure. Briggs et al. (2007) showed that the Irtysh fault was active during two episodes of subduction below the Altai arc: first, in the Ordovician, and second, in the Late Carboniferous and Early Permian. During the second episode the fault constituted a crustal-

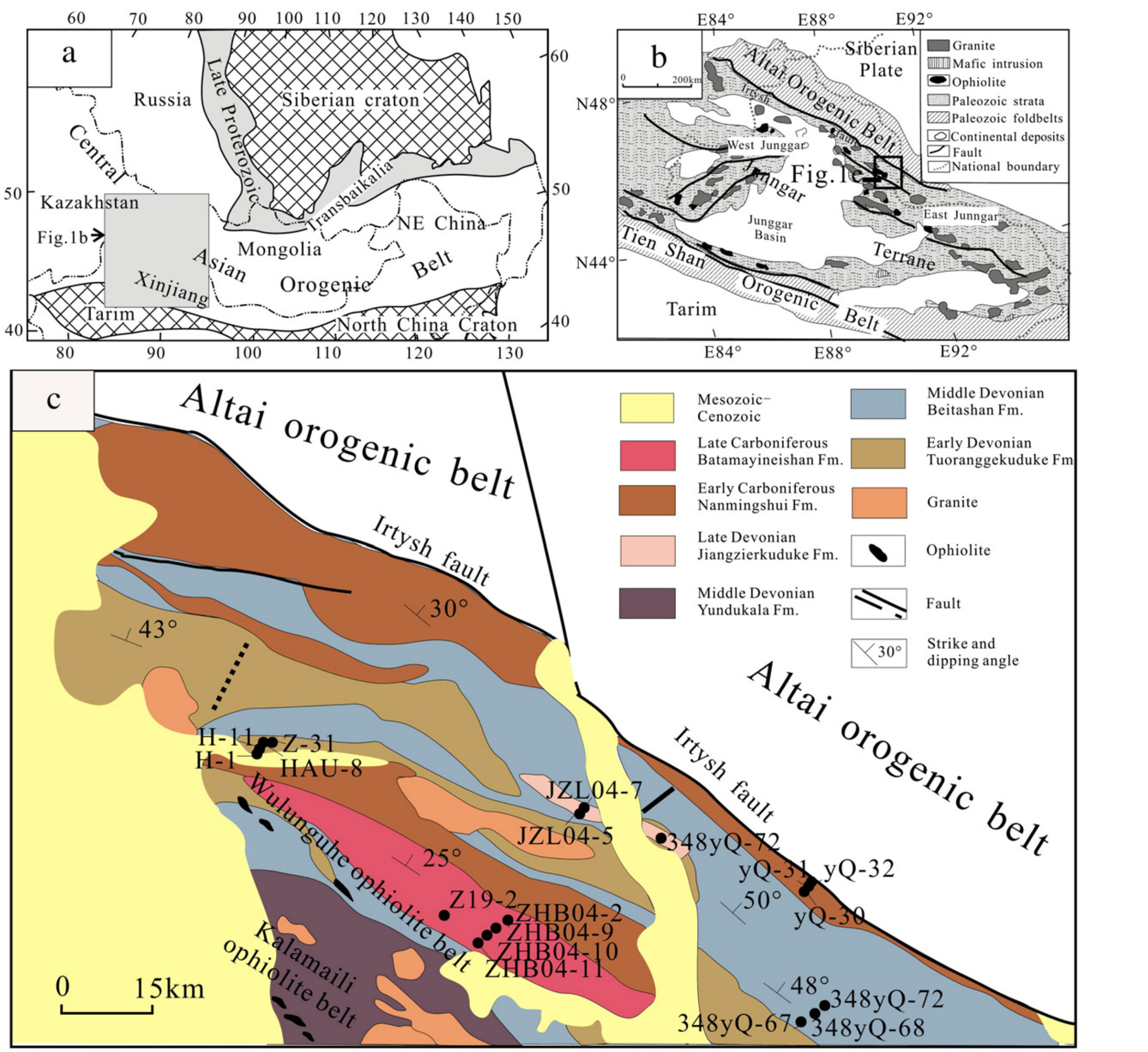

Fig. 1. (a) Relationship of study area with the Central Asia orogenic belt (modified from Jahn et al., 2000); (b) Simplified geological map of the Junggar terrane in northern Xinjiang (modified from Chen and Jahn, 2004); (c) Distribution of Paleozoic volcanic rocks in the Eastern Junggar terrane with sample localities. The geology of the Altai orogenic belt to the north of the Irtysh Fault is not shown. Because of too many samples from the Tuoranggekuduke Fm. and Beitashan Fm., only dashed and solid lines are used to represent the locations of the samples from the two formations.

Please cite this article as: Zhang, Z., et al., Late Paleozoic volcanic record of the Eastern Junggar terrane, Xinjiang, Northwestern China: Major and trace element characteristics, Sr–Nd isotopic systematics and implications ..., Gondwana Research (2009), doi:10.1016/j.gr.2009.03.004

scale thrust during north dipping subduction of the Junggar Ocean below the Altai arc. During this event a mélange complex formed and was underplated below the older Ordovician arc, metamorphosed at lower crustal depths, and then exhumed to the upper crust along the south-directed Irtysh thrust zone. Goldfarb et al. (2003) also suggested that the terranes of the Altai and Junggar regions were amalgamated into a Cordilleran-type orogen by the Early Permian. Windley et al. (2002) pointed out a Devonian–Carboniferous terrane that is interpreted as an island arc (felsic-intermediate volcanic rocks and calc-alkaline plutons) to the south of the Irtysh fault, and that was accreted onto the eastern margin of the Junggar Basin.

The Junggar terrane is traditionally divided into the East and West Junggar terranes and the Junggar Basin. The Junggar basin is filled with about 10 km of continental sedimentary rocks, the oldest of which are Early Permian (Coleman, 1989; Xiao et al., 2008). The nature of the basement beneath the basin has long been controversial because of the paucity of stratigraphic, geochemical and geochronological data. Some workers have interpreted gravitational, aeromagnetic and seismic data to indicate that the basin is floored by ancient continental crust. Consequently, the Junggar basement has been considered to represent a micro-continent of Precambrian age (e.g., Charvet et al., 2007, and references therein). Others interpreted it as a fragment of trapped Paleozoic oceanic crust (Filippova et al., 2001; references in Xiao et al., 2008). The geochemical and Nd isotopic features of igneous rocks cropping out along the basin margins suggest that it is made of a juvenile accretionary crust or an Early Paleozoic volcanic arc (Chen and Jahn, 2004; Jahn, 2004). Recently, Zheng et al. (2007) showed that the elemental and Sr–Nd–Pb isotopic compositions and zircon Pb–Pb ages of volcanic rocks from drill cores through the paleo-weathered crust show that the basement of the Junggar basin is composed mainly of Late Paleozoic volcanic rocks with minor shale and tuff. They argued that the entire Junggar basin has a juvenile but heterogeneous basement that may result from amalgamation of oceanic crustal blocks derived from different terranes and in different stages of evolution. The East Junggar terrane comprises several NW-SE trending, highly deformed metasedimentary and ophiolite assemblages which were accreted to the southern margin of the Siberian craton. The West Junggar terrane (Fig. 1b) was accreted to the Kazakhstan block to the west by the end of Carboniferous time. It is composed of various terranes of arc subduction origin (Windley et al., 1990; Buckman and Aitchison, 2001, 2004). The previous studies on Carboniferous granites in the West Junggar area suggest that they were produced by partial melting of material of oceanic crust with no or minor contribution from Precambrian basement (e.g., Chen and Jahn, 2002, 2004; Chen and Arakawa, 2005).

The East Junggar terrane comprises several accretionary complexes that were generated by subduction–accretion processes in Paleozoic times (Coleman, 1989; Feng et al., 1989). Two highly deformed and dismembered belts of ophiolites, the northern Wulunguhe and the southern Kalamaili ophiolite belts (Fig. 1c), crop out in the Eastern Junggar terrane; the Wulunguhe ophiolite is dated at 481 ± 5 to 489 ± 4 Ma by Jian et al. (2003) using SHRIMP U–Pb zircon methods, whereas the Kalamaili ophiolite was determined to be 373 ± 10 Ma (U–Pb zircon; Tang et al., 2007), 497 ± 12 Ma, 403 ± 9 Ma, 336 ± 4 Ma, and 342 ± 3 Ma (Ping et al., 2005). These ophiolites reflect the formation of oceanic crust in the Early to Middle Paleozoic. Subduction of the oceanic crust beneath the Altai orogen and the Kazakhstan block is manifested by the presence of thick marine volcaniclastics and volcanic flows intercalated with sediments of Devonian to Carboniferous ages. This was followed by accretion and imbrication of the arc series and back-arc basins towards the Kazakhstan block as the three blocks (Tarim, Kazakhstan and Siberian plate) converged. The termination of these oceanic systems during the Carboniferous is indicated by continental deposits that abruptly overlap the earlier Paleozoic marine facies deposits, and Early to Late Devonian–earliest Carboniferous (Tournaisian) radiolarites are unconformably overlain by younger Carboniferous strata (Charvet et al., 2007). Post-collisional magmas, mainly A type granitoids and temporally and spatially associated Cu–Ni bearing mafic and ultramafic plutons intruded into the fold belt (Mao et al., 2008; Zhang et al., 2008a). The recent high-resolution ICP-MS Re–Os dating Cu–Ni sulfides of the Kalatongke intrusion and SHRIMP U–Pb zircon dating on a norite from the intrusion yielded ages of 282.5 ± 4.8 Ma and 290.2 ± 6.9 Ma (Zhang et al., 2008a) and 287 ± 5 Ma (Han et al., 2004) respectively. These ages suggest that the Kalatongke mafic–ultramafic rocks and the Cu–Ni sulfide ores were emplaced during Early Permian times.

The strata outcropping in the East Junggar terrane consist of a Devonian to Early Carboniferous marine volcanic–sedimentary sequence, a Late Carboniferous to Permian continental volcanic–sedimentary sequence and Mesozoic coal-bearing sedimentary rocks. All Paleozoic strata strike northwest, and dip northeast (Fig. 1c). The Late Paleozoic volcanic sequence consists of the Early Devonian Tuoranggekuduke (TK) Formation (Fm.), Middle Devonian Beitashan (BS) Fm., Middle Devonian Yundukala (YK) Fm., Late Devonian Jiangzierkuduke (JK) Fm., Early Carboniferous Nanmingshui (NS) Fm., Late Carboniferous Batamayineishan (BN) Fm. and Early Zaheba (ZB) Fm. from base upward. The Early Devonian Tuoranggekuduke Fm. is the oldest in the Junggar terrane, and the Carboniferous strata are distributed in the northernmost part of the terrane (Fig. 1c). The Early Zaheba Fm. is a suite of continental basalt, andesite and dacite intercalated with tuff and siltstone. The characteristics of other formations are described next.

The Early Devonian Tuoranggekuduke Fm. consists of a 3200 m-thick succession of intermediate-basic to intermediate-acid volcanic rocks, including pyroclastic rocks and siltstone intercalated with intermediate-basic lavas in the lower part of the formation, intermediate-basic lavas intercalated with tuff in the middle part, and tuff with tuffaceous sandstone intercalated with siltstone and basalt in the upper part of the formation. In addition, minor felsic lavas are locally recognized. Zhang et al. (2006) proposed that the SHRIMP U–Pb age (408 ± 9 Ma) of the xenocrystic zircon grains from the granodiorite porphyry intrude the overlying strata (the Beitashan Fm.) represent the age of the Tuoranggekuduke Fm. volcanic rocks.

The Beitashan Fm. can be divided into three parts from base to top. The lower part consists of basalt, basaltic tuff, basaltic breccia, picrite and ankaramite, and one 2–20 m thick magnetite layer, which is believed to be sedimentary in origin, deposited during a period of volcanic activity (Yan et al., 2005). Ankaramite flows are located at the top of the lower part of the formation. The ankaramite flow is 5–10 m thick, and it is interbedded with basaltic lavas. There is no clear boundary between ankaramite and basalt, and it is not associated with the picritic flow. The picritic flow succession becomes thicker toward the southeast, from a total ~100 m to 2 m. The succession includes 8–15 flows with individual thickness of 2 to 7 m. The basalts comprise intercalated massive aphyric and minor pyroxene-phyric flows. The middle part of the formation is composed of aphyric basalts alternating with pyroxene-phyric basalts, each flow is 2–10 m thick. The upper part of the formation comprises approximately 300 m of andesitic lava flows. The upper part of the formation also includes sedimentary tuff, chert, siltstone and sandstone. Although the isotopic age of the Beitashan Fm. has not been reported, it can be inferred that it formed in the Middle Devonian based on the following evidence. First, the fossils in the Beitashan Fm., including Brachiopoda (*Mucrospirifer mucronatus*, *Acrospirifer* sp., *Tridensills* p., *Spinatrypa* sp.), Bryozoa (*Fenestella* sp.) and plant fossils (*Lepidosigillaria*), indicate a Middle Devonian age (385–398 Ma, Gradstein et al., 2004). Second, Zhang et al. (2006) obtained SHRIMP U–Pb zircon ages of 376 ± 10 to 381 ± 6 Ma from granitic porphyries that intrude the Beitashan Fm. Thus, it can be inferred that the Beitashan Fm. is Middle Devonian in age.

The Middle Devonian Yundukala Fm. is a suite of shallow marine fine clastic rocks intercalated with intermediate rocks and basic rocks.

It can be divided into three parts. The lower part is composed of pyroclastic rocks, siltstone intercalated intermediate-basic lavas, and the middle part comprises intermediate-basic lavas with intercalated tuffs, whereas the upper part consists of tuff and tuffaceous sandstone intercalated with siltstone and basalt.

The Late Devonian Jiangzierkuduke Fm. includes a succession of pyroclastic rocks (dominated by tuff) interbedded sandstone, basaltic andesite, andesite and dacite.

The Early Carboniferous Nanmingshui Fm. is a succession of volcanic–sedimentary rocks. However, the formation consists of various types of rocks in different areas. In some areas, the formation is composed of basaltic tuff, black shale and chert intercalated with pillow basalt. In the Kalatongke Cu–Ni deposit, the formation comprises >450 m thick red argillaceous sandstone, argillite, and grayish green tuffaceous slate with limestone and chert in the lower part, gray-grayish yellow sedimentary–volcanic breccia and dark gray carbonaceous tuff with andesite and tuffaceous chert in the middle, and grayish yellow sedimentary tuff, dark gray carbonaceous slate and minor limestone with basalt and basaltic andesite in the upper part.

The Late Carboniferous Batamayineishan Fm. consists dominantly of basalt and basaltic andesite, locally with minor interbedded andesite, rhyolite, tuff, siltstone and carbonaceous shale. All volcanic rocks have gray and light red colors. Unlike those from the other formations, the lavas exhibit dramatically variable thickness and cover small areas, indicating that they formed in a continental environment rather than in a marine environment. The fossils in the Batamayineishan Fm., including *Angaropteridium* cf. *Cordiopteroides* (*Schmain., Zai*), *Noggerothiopsis* sp., *N.* cf. *Theodori Tschirkovaet Zalossky*, *N. subangusta Zalessky*, *Calamites* sp. (Zhu et al., 2005), indicate a continental setting and a Late Carboniferous age (290–318 Ma, Gradstein et al., 2004), which is consistent with the 309 Ma age by whole-rock K–Ar dating on a felsic sample (Yang et al., 2001).

3. Petrography

Although the lavas from different formations have the same bulk rock types, they have distinct petrographic characteristics. Here, we describe the petrography of the main rock types from these formations that have been analysed in this paper.

3.1. Tuoranggekuduke Fm.

Basalts are porphyritic with 10–20 vol.% phenocrysts consisting predominantly of clinopyroxene and subordinate plagioclase. Clinopyroxene phenocrysts are euhedral, up to 5 mm across, and some of them have been partly replaced by chlorite and epidote, but most of them are fresh. The plagioclase phenocrysts are subhedral, long column-shaped, and some of them have been completely replaced by albite. The groundmass consists chiefly of clinopyroxene and plagioclase, with minor interstitial anhedral granular magnetite.

Andesites are also porphyritic. They contain less than 5 vol.% phenocrysts in an interstitial groundmass. Phenocryst phases are subhedral plagioclase and minor clinopyroxene. The groundmass has pilotaxitic texture, and comprises plagioclase (~80 vol.%) and minor small granular clinopyroxene and magnetite. The rocks have been affected by extensive alteration with primary minerals replaced by sericite, chlorite and clay minerals.

Dacites contain minor plagioclase, biotite and quartz phenocrysts (<5 vol.%) in a pilotaxitic matrix of microcrystal plagioclase (70 vol.%), quartz (5 vol.%) and some glass. Some plagioclases have been extensively altered to sericite.

3.2. Beitashan Fm.

Picritic and ankaramitic rocks are highly porphyritic. Phenocryst assemblages in picrites are olivine (up to 30 vol.%) and minor Cr-spinel, embedded in a matrix of groundmass granular olivine, clinopyroxene and minor plagioclase and Fe–Ti oxides. Most olivine phenocrysts are replaced by serpentine, but most grains retain cores of unaltered olivine. Some of them contain scattered melt inclusions. Olivine phenocrysts are typically 0.5–1 mm in diameter but rarely exceed 2 mm. Glass does not appear to be preserved. Minor small sulfides are scattered in the groundmass and in some cases included in clinopyroxene phenocrysts. The dominant phenocryst phase in ankaramites is clinopyroxene, with subordinate olivine. The phenocrysts account for about 10–15 vol.% of the rock. Clinopyroxene phenocrysts are relatively fresh, short, column-shaped, and some of them have been replaced by chlorite. Olivine phenocrysts are everywhere replaced by epidote and actinolite, and only their outlines are retained. The groundmass consists chiefly of clinopyroxene, plagioclase, with minor scattered magnetite and metal sulfides. In addition, minor small Cr-spinel crystals (10–50 μm) are included in clinopyroxene phenocrysts.

The basalts are porphyritic with variable amounts of phenocrysts of clinopyroxene and plagioclase in a matrix of plagioclase, clinopyroxene and irregular granular magnetite. Clinopyroxene phenocrysts are euhedral to subhedral, and some of them have been partly replaced by epidote, chlorite and actinolite. However, some grains remain fresh. They also contain Cr-spinel. Plagioclase phenocrysts are subhedral tabular-shaped, 0.5–1.5 mm long, and most of them are replaced by albite. Some basalts have amygdaloidal chlorite, epidote and calcite. Calcite rarely occurs as veinlets. Thus, high volatile contents in the rocks can be attributed to alteration and low-grade metamorphism.

The andesites are porphyritic, with a few phenocrysts of plagioclase and amphibole in a pilotaxitic matrix of plagioclase and minor magnetite. The andesites have been extensively altered with primary minerals largely replaced by sericite, chlorite and clay minerals.

3.3. Yundukala Fm.

Basalts, appearing dark green, are porphyritic with 5–10 vol.% phenocrysts of plagioclase and dark minerals in a matrix of microcrystalline plagioclase (50 vol.%) and clinopyroxene (40 vol.%) with minor intergranular anhedral magnetite (<5 vol.%). Plagioclase phenocrysts are platy-shaped, 0.2–0.8 mm across, and typically replaced by albite. However, almost all dark mineral phenocrysts have been replaced by chlorite. The groundmass has been partly altered by carbonate minerals.

3.4. Jiangzierkuduke Fm.

Basalts are porphyritic. Some lavas are vesicular (1–2 vol.%) and contain less than 5 vol.% phenocrysts in an interstitial groundmass. Phenocryst phases are idiomorphic clinopyroxene and subhedral plagioclase. The groundmass consists of plagioclase, clinopyroxene and insterstitial opaques, all smaller than 0.05 mm in diameter. Some clinopyroxene phenocrysts have been replaced by chlorite, epidote and actinolite, and plagioclase phenocrysts have been replaced by sericite. Comparably, the groundmass remains relatively fresh, locally replaced by calcite.

3.5. Nanmingshui Fm.

Due to the effect of the Irtylish fault, the basalts have been pervasively metamorphosed. However, phenocrysts and groundmass can be distinguished. The rock contains about 15 vol.% phenocrysts, which consist predominantly of dark minerals and plagioclase. The dark minerals have been completely replaced by amphibole and epidote, and only outline of clinopyroxene is preserved. The groundmass comprises short column-shaped plagioclase and interstitial anhedral magnetite and granular clinopyroxene replaced by amphibole.

Please cite this article as: Zhang, Z., et al., Late Paleozoic volcanic record of the Eastern Junggar terrane, Xinjiang, Northwestern China: Major and trace element characteristics, Sr–Nd isotopic systematics and implications ..., Gondwana Research (2009), doi:10.1016/j.gr.2009.03.004

3.6. Batamayineishan Fm.

Basalt and basaltic andesite have the same mineral assemblage and texture, and cannot be easily distinguished in hand specimen, but basalt has much higher contents of clinopyroxene. The rocks are vesicular (5–10 vol.%), and porphyritic with 5–15 vol.% phenocrysts of subhedral column-shaped plagioclase and minor subhendral clinopyroxene. The groundmass consists predominantly of microcrystalline column-shaped plagioclase (70 vol.%) and interstitial granular clinopyroxene (20 vol.%) and minor magnetite (<1 vol.%). All rocks are relatively fresh, and no obvious alteration has been recognized.

4. Analytical methods

Representative samples for major element, trace element and isotopic analyses were reduced to chips after removal of altered surfaces. The chips were then pulverized into powders using agate mortars.

Bulk-rock major and trace element compositions were determined at the Chinese Academy of Geological Sciences. Major element determinations were done by an X-ray fluorescence spectrometer using the methods of Norrish and Chappel (1977), and ferrous iron was determined by a wet chemical method. The trace element abundances were determined by inductively coupled plasma-mass spectrometry (ICP-MS) following Dulski (1994). The precision of the analyses was generally ~1% for major oxides, ~0.5% for SiO_2, and 3–7% for trace elements. Accuracy values are based on the average of repeated analysis of standard BHVO-1.

The isotope ratios of Nd and Sr and associated isotope-dilution concentrations were measured at the Chinese Academy of Sciences on small, handpicked chips of acid-cleaned rock in order to avoid alteration and olivine phenocrysts (e.g., Peng and Mahoney, 1995). The analytical procedures followed Harmer et al. (1986). $^{87}Sr/^{86}Sr$ and $^{143}Nd/^{144}Nd$ ratios were determined on a VG 354 mass spectrometer, and isotopic ratios were normalized to $^{145}Nd/^{144}Nd = 0.7219$ and $^{86}Sr/^{88}Sr = 0.1194$. Repeated analyses of standards yielded averages of 0.710245 ± 0.000018 (2σ, $n = 6$) for Sr standard NIST SRM987, and 0.511870 ± 0.000018 (2σ, $n = 6$) for the LaJolla Nd standard. Total chemical blanks were <200 pg for Sr and <100 pg for Nd.

5. Results

Representative samples from the Late Paleozoic volcanic rocks including the Early Devonian YK Fm., Middle Devonian BS Fm., Middle Devonian YK Fm., Late Devonian JK Fm., Early Carboniferous NS Fm. and Late Carboniferous BN Fm. were chosen to analyze their major and trace element compositions as well as their Sr and Nd isotopic compositions. The results are listed in Tables 1 and 2.

5.1. Alteration effects

It is necessary to understand the mobility of elements during low-temperature alteration before using them to assess the primary compositions of the magmas. Except for the BN Fm., the Paleozoic volcanic rocks from other formations in the Eastern Junggar terrane have undergone weak alteration as indicated by their weight loss on ignition (Table 1) and petrographic characteristics. Previous studies have suggested that under such metamorphic conditions and alteration types, Fe, Al, Ca and Mg, Cu and Ni are relatively immobile, while K, Na, Rb, Sr and Ba are typically mobile (Beswick, 1982). Therefore $(^{87}Sr/^{86}Sr)_t$ ratios may also likely reflect the alteration effects. However, high field strength elements (HFSEs), such as Nb, Ta, Zr, Hf, Th, Ti, Y and REE including Sm–Nd isotopic system may have remained immobile (Barnes et al., 1985). Hence, it can be inferred that major elements Fe, Al, Ca and Mg, HFSEs coupled with $\varepsilon_{Nd}(t)$ values may not have been affected by alteration, and can reflect those of the original magmatic rocks.

5.2. Major elements

Because the Late Paleozoic rocks in the Junggar terrane have undergone various extents of low-temperature alteration, and K and Na are typically mobile, the TAS diagram (Le Maitre, 1989) cannot be used for nomenclature of the rocks. Thus, their rock names used here are solely based on their SiO_2 contents.

As a whole, the lavas from the TK, BS and YK Fms. have similar major element compositions, which are characterized by relatively low TiO_2 (generally <1.5 wt.%) and high Al_2O_3 contents (generally >17 wt.% for basalts). In contrast, those from the JK, NS and BN Fms. have relatively high TiO_2 (generally >1.7 wt.%) and low Al_2O_3 contents (<17 wt.%). From the Early Devonian TK Fm. to Late Carboniferous BN Fm., they display a trend of increasing TiO_2 contents at the same SiO_2 (Fig. 2). Except for the picrites and ankaramites from the BS Fm., all other samples have low Mg# [Mg/(Mg + Fe)] values, which indicate that they were derived from relatively evolved magmas. Comparably, the lavas from the NS Fm. have SiO_2 contents <49 wt.%, indicating that they are basalts, which have relatively high MgO (7.8–8.3 wt.%) and CaO contents (9.2–10.3 wt.%).

5.3. Trace elements

The Late Paleozoic volcanic rocks from the Eastern Junggar terrane have distinctive rare earth element (REE) compositions. As expected from the low distribution coefficients of REE, the felsic rocks have the highest REE concentrations, and the ultramafic rocks (e.g., picrites) have the lowest REE concentrations. However, the basaltic rocks from the different formations exhibit various REE concentrations and light REE/high REE ratios. The TK Fm. has total REE concentrations ranging from 48 to 132 ppm, 25 to 133 ppm for the BS Fm. except for one basaltic andesite sample, 67 to 90 ppm for the YK Fm., and 71 to 102 ppm for the NS Fm. Comparably, the JK and BN Fms. have higher REE contents, 202 to 214 ppm and 132 to 245 ppm. In addition, these two formations also have higher $(La/Yb)n$ ratios, 5.6 to 6.8 and 3.4 to 8.2 respectively, whereas the NS Fm. has the lowest $(La/Yb)n$ ratios, from 2.3 to 2.8.

Except for the picrites from the BS Fm. with high Cr and Ni contents, other rocks have relatively low Cr and Ni contents. For comparison, only basalts and basaltic andesites from the different formations are plotted on primitive mantle-normalized trace element patterns. Among the trace elements, Rb and Ba are considerably variable relative to alteration-resistant elements such as Th and Nb, so only alteration-resistant elements are plotted in Fig. 3. Except for the NS Fm., the lavas from all other five formations are enriched in more highly incompatible elements relative to moderately incompatible ones. In contrast, the basalts from the NS Fm. exhibit a similar even shape with relatively low incompatible element concentrations (Fig. 3). All lavas show variably negative Nb, Ta and Ti anomalies, which are characteristic of subduction-related volcanic rocks. However, the negative Nb, Ta and Ti anomalies tend to decrease from the Early Devonian TK Fm. to Late Carboniferous BN Fm., in which the lavas display very slightly negative Nb anomalies with moderately negative Ti anomalies. Except for the TK Fm., significant troughs at Y are present in the lavas from other formations. In addition, large peaks in Sr are also present in many of the primitive mantle-normalized element patterns in Fig. 3, and Sr does not correlate with the alteration-resistant element Eu, which is also compatible in plagioclase. Thus, Sr concentrations appear to have been affected considerably by alteration, as has been documented in altered subaerial basalts elsewhere (e.g., Lindstrom and Haskin, 1981; Clague and Frey, 1982; Fleming et al., 1992).

5.4. Sr–Nd isotopes

Because the volcanic rocks formed in Late Paleozoic time, we must make an age-correction for Sr and Nd isotopes before we use them to

Please cite this article as: Zhang, Z., et al., Late Paleozoic volcanic record of the Eastern Junggar terrane, Xinjiang, Northwestern China: Major and trace element characteristics, Sr–Nd isotopic systematics and implications ..., Gondwana Research (2009), doi:10.1016/j.gr.2009.03.004

Table 1
Major and trace element analyses for bulk rocks.

Sample	H-1	H-11	HAU-8	Z-31	A0122	A0322	A0623	A1022	D36	D47	D314	D324	Z303
Rock	D	D	D	A	BA	BA	BA	A	B	B	BA	B	BA
Formation	Tuoranggekuduke												
SiO_2	62.12	62.88	61.67	56.75	54.92	55.93	55.13	57.03	48.94	53.14	55.71	47.21	51.84
TiO_2	0.51	0.59	0.51	1.00	0.76	0.99	0.78	0.67	1.33	0.82	1.04	1.60	0.73
Al_2O_3	16.69	14.87	17.68	14.48	18.17	15.13	16.17	17.42	15.19	13.17	18.28	17.79	16.68
Fe_2O_3	1.65	1.95	4.63	1.39	6.45	7.81	4.55	4.35	4.89	4.48	1.46	5.75	4.55
FeO	2.34	2.73	1.57	4.64	1.83	2.91	4.22	3.11	5.55	4.60	4.79	6.09	5.35
MnO	0.09	0.12	0.14	0.16	0.14	0.16	0.16	0.12	0.18	0.13	0.17	0.21	0.21
MgO	1.84	1.67	2.42	5.28	3.88	4.96	4.96	3.03	5.55	7.22	13.20	5.41	7.90
CaO	8.64	4.53	4.26	5.19	4.98	4.12	4.69	6.27	10.08	9.04	4.02	9.31	6.69
Na_2O	3.44	3.86	3.86	4.84	4.82	3.95	5.20	4.41	3.25	3.33	0.96	3.56	1.59
K_2O	0.25	1.84	2.69	3.61	1.64	1.28	1.09	1.07	1.42	1.77	0.25	2.06	0.53
P_2O_5	0.17	0.24	0.21	0.38	0.22	0.16	0.25	0.23	0.39	0.50	0.00	0.33	0.14
LOI	2.23	4.67	0.35	2.28	2.17	2.6	2.79	2.32	3.19	1.78	0.12	0.69	3.78
Mg#	50.70	44.40	47.39	65.72	52.04	51.63	56.08	48.00	54.40	64.16	82.23	50.67	64.15
La	9.94	16.09	16.52	28.96	15.46	13.77	17.89	14.27	14.94	13.26	20.04	18.54	10.34
Ce	18.79	27.40	31.98	56.33	32.28	28.66	36.90	29.40	27.70	26.40	42.80	40.90	26.00
Pr	2.53			7.15	4.43	3.98	4.76	3.87					
Nd	8.65	11.00	21.00	25.25	19.11	17.37	20.20	16.76	16.00	14.00	19.90	18.20	13.50
Sm	1.87	2.09	3.14	4.51	3.99	3.67	4.28	3.51	4.23	3.15	4.38	5.21	2.34
Eu	0.57	0.68	0.90	1.17	1.17	1.06	1.25	1.02	1.42	1.09	1.29	1.80	0.89
Gd	1.59			3.13	3.68	3.39	4.19	3.57					
Tb	0.27	0.28	0.42	0.48	0.521	0.48	0.59	0.51	0.43	0.44	0.65	1.07	0.31
Dy	1.47			2.10	2.99	2.68	3.40	2.87					
Ho	0.29			0.39	0.59	0.53	0.67	0.59					
Er	0.86			1.04	1.58	1.37	1.76	1.73					
Tm	0.13			0.15	0.25	0.21	0.28	0.27					
Yb	0.88	0.66	0.82	0.86	1.65	1.37	1.86	1.70	1.23	1.19	0.94	1.08	0.46
Lu	0.13	0.09	0.07	0.12	0.27	0.21	0.29	0.27	0.25	0.15	0.11	0.12	0.08
Ba	550	734	1285	1250	784	551	507	688	741	799	425	481	643
Cu													
Sr	565	560	757	879	1813	1050	503	720	713	720	776	636	602
V	80.0	60.0	138.0	140.0	211.4	256.6	200.4	203.5	250.0	270.0	194.0	299.0	220.0
Zn													
Co	5.00	5.00	29.00	10.00	22.90	33.49	25.45	17.44	5.00	5.00	18.00	34.00	42.00
Ga													
Pb													
Rb		36.00	26.00		25.48	18.82	16.26	13.40	10.60	37.00	18.50	48.90	13.80
Sc	9.0	8.0	17.0	14.0									
Th		4.00	4.40		2.84	1.81	2.86	2.46	1.60	3.20	3.40	1.10	2.70
U			1.60		1.32	1.43	1.56	1.25			1.30	0.90	0.80
Cr	32	17	22	99	28.77	102	62	32	60	26	45	22	137
Ni	78	39	97	118	12	29	23	15	78	39	131	142	216
Zr	90	115	124	137	97	79	94	82	86	66	127	155	78
Nb	5.0	12.0	4.0	15.4	3.5	3.1	5.1	3.5	16.0	13.0	8.0	9.0	6.0
Hf		2.92	2.84		2.84	2.37	2.67	2.19	2.53	2.32	2.96	3.1	2.41
Ta		0.95	0.23		0.24	0.17	0.31	0.2	0.4	0.22	0.289	0.13	0.458
Y	8.00	13.00	18.00	10.00	15.55	13.77	17.62	17.97	28.00	21.00	31.00	40.00	23.00
Reference	Xu et al. (2001)				Mei et al. (1993)								
Sample	XJ21-17	20,004	LTS03-5	20,020	SJ04-21	SJ04-22	20,005	20,012	XJ21-20	yQ-78	KLX-45	yQ-79	yQ-82
Rock	B	B	P	P	P	P	P	P	P	B	B	B	A
Formation	Beitashan												
SiO_2	48.72	49.19	47.85	47.20	46.01	48.26	47.44	47.35	45.92	48.5	49.19	52.25	60.94
TiO_2	1.50	1.14	0.42	0.45	0.48	0.43	0.42	0.49	0.71	0.63	0.86	0.91	0.63
Al_2O_3	16.67	15.33	7.47	6.45	7.9	7.06	9.16	6.77	8.67	20.24	18.1	18.94	18.26
Fe_2O_3	3.11	4.13	4.19	5.32	7.1	5.88	3.69	5.92	5.15	1.97	10.59	1.98	0.82
FeO	6.89	9.08	7.69	6.26	4.96	4.56	6.58	5.67	6.37	9.84	1.88	9.88	4.08
MnO	0.23	0.21	0.21	0.17	0.19	0.16	0.17	0.18	0.25	0.2	0.11	0.23	0.13
MgO	11.05	6.26	21.97	25.12	22.75	24.08	22.22	23.36	21.56	9.17	3.08	5.11	1.65
CaO	10.56	8.37	9.29	7.31	9.64	8.42	9.42	9.44	10.46	3.52	10.43	4.67	3.13
Na_2O	0.63	3.18	0.44	1.26	0.44	0.61	0.56	0.4	0.5	5.02	3.27	4.89	4.5
K_2O	0.31	2.77	0.2	0.23	0.17	0.29	0.11	0.18	0.16	0.82	2.05	0.72	5.57
P_2O_5	0.33	0.34	0.28	0.23	0.35	0.24	0.23	0.24	0.26	0.1	0.42	0.42	0.29
LOI	5.71	2.17	4.4	2.31	4.09	5.01	3.07	4.62	3.62	6.12	2.67	3.93	2.25
Mg#	72	52	81	84	82	84	83	83	81	64	38	49	43
La	6.83	8.28	4.70	4.45	5.69	3.69	5.60	5.18	3.85	4.89	13.90	16.00	11.10
Ce	15.99	15.40	10.80	8.58	11.96	7.74	9.20	8.66	8.68	8.07	28.30	27.60	20.60
Pr	2.36	2.34	1.59	1.02	1.72	1.14	1.28	1.50	1.34	1.04	3.58	3.96	3.20
Nd	11.40	12.30	7.61	5.56	8.61	5.79	5.95	6.08	6.47	5.35	15.80	17.50	14.90
Sm	3.64	3.51	2.01	1.58	2.45	1.53	1.66	1.54	1.90	1.37	3.79	3.98	3.54
Eu	1.35	1.14	0.65	0.54	0.64	0.46	0.56	0.53	0.53	0.65	0.93	1.2	1.17
Gd	4.66	3.53	1.89	1.70	2.17	1.65	1.79	1.42	2.23	1.79	3.58	3.73	3.76
Tb	0.82	0.68	0.28	0.28	0.32	0.26	0.31	0.26	0.41	0.31	0.60	0.64	0.68

Table 1 (*continued*)

Sample	XJ21-17	20,004	LTS03-5	20,020	SJ04-21	SJ04-22	20,005	20,012	XJ21-20	yQ-78	KLX-45	yQ-79	yQ-82
Rock	B	B	P	P	P	P	P	P	P	B	B	B	A
Formation	Beitashan												
Dy	5.45	4.60	1.65	1.82	1.99	1.60	1.93	1.7	2.66	2.33	3.75	4.20	4.43
Ho	1.18	0.89	0.33	0.35	0.43	0.34	0.38	0.38	0.57	0.42	0.75	0.78	0.84
Er	3.34	2.68	0.90	0.96	1.09	0.92	1.02	1.00	1.63	1.35	2.23	2.36	2.58
Tm	0.50	0.42	0.13	0.14	0.17	0.14	0.14	0.14	0.25	0.20	0.32	0.32	0.36
Yb	3.15	2.63	0.85	0.84	1.16	0.99	0.98	0.90	1.60	1.18	2.02	1.85	2.07
Lu	0.47	0.34	0.13	0.12	0.16	0.13	0.13	0.12	0.25	0.16	0.3	0.24	0.26
Ba	1654	858	15	81	103	184	38	72	36	345	273	314	3950
Cu	25.0		55.5		8.9	36.9			27.8		6900		
Sr	312	570	83.3	382	178	207	54	176	129	443	1506	342	88
V	263	440	175	222			190	182	276	1330	280	1300	1230
Zn	81.81		66.50		74.20	76.70			66.62		32.90		
Co	36.2	39.5	76.4	66.3	72.3	78.9	66.9	72.3	57.43	39.4	33.9	23.9	4.2
Ga	10.32	26	9.49	12.8	7.7	8.15	14.8	14.6	6.82	31.2	41.9	33.5	25.8
Pb	13.02		1.27		1.85	2.08			2.772		12.5		
Rb	4.13	44	5.55	5.8	2.9	5.28	2.15	7.3	4.81	14.3	37.3	10.3	69.2
Sc	42.18		18.1		24.1	24			47.56		26.1		
Th	0.588		0.430		0.620	0.410			0.653		1.870		
U	0.28	1.46	0.34	1.08	0.31	0.31	1.00	1.00	0.25	1.03	1.52	0.80	1.03
Cr	184	111	1241	1260			1040	1380	404	13.5	127	16.4	5.1
Ni	51	29.2	555	880	519	805	840	773	171	25.4	52.7	18.6	7.8
Zr	82.5	106.0	30.6	77.5	23.6	20.2	37.2	72.7	36.9	66.2	74.8	140.0	84.4
Nb	6.12	3.73	1.03	1.08	1.78	2.60	2.46	1.06	2.71	1.45	3.47	4.59	5.32
Hf	2.559	4.74	0.67	2.01	0.77	0.65	1.89	2.29	1.09	2.06	2.17	4.49	2.69
Ta	0.397	<0.5	0.21	<0.5	0.25	0.24	<0.5	<0.5	0.159	<0.5	0.25	<0.5	<0.5
Y	28.43		8.68		8.84	7.87			14.39	9.49	17	16.2	18.1
Reference	This study												

Sample	yQ-83	LS03-13	yQ-84	YQ-102	yQ-85	XJ22-8	yQ-94	yQ-96	XJ23-18	KLX-42	XJ21-22	SJ04-29	XJ22-10
Rock	BA	A	B	B	BA	A	BA	BA	BA	BA	P	P	BA
Formation	Beitashan												
SiO_2	54.72	58.45	49.33	49.74	55.54	57.53	55.11	56.12	54.45	55.26	47.73	48.41	52.12
TiO_2	0.91	0.49	0.71	1.10	0.94	0.67	2.04	1.28	0.72	0.33	0.48	0.61	0.44
Al_2O_3	16.57	17.92	18.95	17.43	16.50	19.22	17.01	17.16	16.50	13.39	8.33	7.34	10.86
Fe_2O_3	1.80	3.97	1.81	1.86	1.38	3.36	1.83	1.70	4.57	17.00	2.21	3.17	8.34
FeO	8.98	2.78	9.07	9.31	6.89	4.51	9.11	8.47	4.90	4.35	8.57	7.15	2.99
MnO	0.18	0.13	0.17	0.18	0.14	0.25	0.16	0.16	0.20	0.05	0.26	0.19	0.24
MgO	4.01	2.18	6.34	6.29	4.44	2.28	3.90	1.47	5.35	1.24	25.15	22.86	8.11
CaO	6.46	3.92	9.94	4.81	5.98	4.38	3.24	3.05	3.74	0.35	6.68	8.92	9.96
Na_2O	4.33	8.18	3.44	3.55	4.32	6.85	6.93	6.46	2.06	2.33	0.25	0.69	3.98
K_2O	1.76	1.55	0.13	5.18	3.41	0.46	0.22	3.61	7.12	5.48	0.10	0.34	2.44
P_2O_5	0.29	0.42	0.12	0.54	0.44	0.49	0.46	0.52	0.39	0.21	0.25	0.31	0.53
LOI	3.08	2.69	6.26	4.83	2.38	2.08	4.7	2.78	1.83	3.30	3.01	3.27	2.93
Mg#	46	43	55	54	55	40	45	25	57	12	84	84	63
La	17.30	11.10	3.90	11.20	23.50	8.96	19.60	59.50		6.24	4.57	5.57	3.28
Ce	31.10	24.50	7.14	20.50	43.70	13.17	39.80	114.00		12.40	9.88	11.16	6.79
Pr	4.54	3.21	1.16	3.20	5.48	2.62	6.18	14.50		1.50	1.51	1.53	1.01
Nd	19.50	14.00	6.00	14.90	24.60	11.24	27.20	60.20		6.67	7.06	7.63	4.87
Sm	4.52	3.25	1.76	3.77	5.04	2.69	6.95	12.70		1.56	1.94	2.10	1.47
Eu	1.51	1.04	0.69	1.22	1.58	0.88	2.03	3.63		0.39	0.44	0.77	0.55
Gd	4.11	3.21	1.94	3.31	4.63	2.70	7.12	10.80		1.50	1.97	2.34	1.79
Tb	0.71	0.50	0.35	0.54	0.65	0.45	1.31	1.87		0.23	0.33	0.39	0.31
Dy	4.78	3.16	2.56	3.65	4.22	2.69	9.16	12.5		1.39	2.1	2.35	1.97
Ho	0.94	0.67	0.49	0.68	0.73	0.54	1.89	2.54		0.27	0.44	0.53	0.4
Er	2.90	1.93	1.48	2.00	2.18	1.59	5.30	6.59		0.80	1.25	1.38	1.15
Tm	0.41	0.27	0.2	0.26	0.29	0.25	0.75	0.96		0.12	0.19	0.21	0.18
Yb	2.60	1.76	1.14	1.55	1.70	1.63	4.68	5.97		0.84	1.31	1.39	1.18
Lu	0.36	0.26	0.14	0.22	0.22	0.25	0.53	0.77		0.12	0.2	0.21	0.17
Ba	1310	492	134	1620	890	313	178	496		718	109	254.1	339
Cu		19.10				105.57				1270.00	13.47	22.30	54.75
Sr	336	202	392	333	221	488	151	15		214	54	292	217
V	613.0	90.9	674.0	406.0	1180.0	129.1	280.0	367.0		100.0	208.1		197.5
Zn		87.4				53.9				52.6	75.0	57.7	56.7
Co	24.6	16.2	36.2	31.3	25.2	13.8	22.8	7.5		39.8	70.9	64.5	41.9
Ga	32.7	19.6	29.4	27.6	30.2	18.2	31.8	38.2		19.9	8.6	7.8	9.2
Pb		5.42				6.15				8.80	1.90	3.22	4.17
Rb	24.4	18.5	3.25	79.9	69.9		4.5	30.1		68.6	4.5	7.1	18.3
Sc		8.08				3.45				7.28	26.23	32.3	44.08
Th		0.96				1.93				1.84	0.79	0.62	0.51
U	0.80	0.37	0.80	1.03	1.48	1.05	0.86	0.92		0.98	0.29	0.42	0.64
Cr	7.32	6.92	14.40	52.00	79.90	45.95	6.24	3.83		35.00	675.37		435.97
Ni	11.6	4.5	19.4	24.9	23.0	20.9	2.8	1.0		24.6	562.0	359.0	125.0
Zr	85.5	62.2	50.0	58.2	148.0	101.8	145.0	53.7		77.7	30.9	30.9	24.8

(continued on next page)

Table 1 (*continued*)

Sample	yQ-83	LS03-13	yQ-84	YQ-102	yQ-85	XJ22-8	yQ-94	yQ-96	XJ23-18	KLX-42	XJ21-22	SJ04-29	XJ22-10
Rock	BA	A	B	B	BA	A	BA	BA	BA	BA	P	P	BA
Formation	Beitashan												
Nb	3.19	2.66	1.49	2.84	8.26	5.12	11.60	51.20		2.11	2.39	2.35	1.96
Hf	3.09	1.82	1.53	2.15	4.39	2.813	4.38	12.50		2.18	0.88	0.95	0.8
Ta	<0.5	0.21	<0.5	<0.5	<0.5	0.326	0.99	3.58		0.2	0.135	0.38	0.11
Y	21.4	16.7	9.82	14.5	15.9	12.7	38.8	50.0		8.6	11.1	11.6	10.3
Reference	This study												

Sample	XJ22-12	YQ-4	LS03-4	LS03-6	XJ20-6	XJ23-14	XJ23-17-1	LS03-7	LS03-8	HLS-11	yQ-76	348yQ-67	348yQ-72
Rock	BA	B	ANK	ANK	ANK	ANK	ANK	B	B	BA	B	B	B
Formation	Beitashan											Yundukala	
SiO_2	53.71	49.19	49.72	49.65	50.54	50.66	51.74	49.25	50.41	52.93	51.16	50.04	47.34
TiO_2	0.50	1.140	0.48	0.49	0.41	0.50	0.41	1.14	1.26	0.75	0.93	1.27	1.68
Al_2O_3	12.49	15.33	9.84	10.25	8.96	9.51	8.39	16.15	17.30	13.43	18.72	17.44	15.75
Fe_2O_3	6.68	2.20	5.04	5.06	3.05	3.90	3.08	4.69	4.75	3.75	9.00	1.69	1.77
FeO	4.37	11.01	6.01	5.64	7.59	5.82	6.57	5.96	5.94	5.84	1.80	8.48	8.84
MnO	0.20	0.21	0.20	0.19	0.20	0.21	0.21	0.18	0.17	0.20	0.14	0.15	0.18
MgO	6.79	6.26	15.46	15.74	17.54	16.64	18.05	9.53	7.93	8.60	5.70	5.81	8.85
CaO	8.13	8.37	10.24	9.86	9.14	10.03	8.82	7.03	4.79	9.01	7.65	8.24	9.03
Na_2O	4.95	3.18	1.90	1.67	0.48	1.64	1.22	3.12	3.53	3.51	3.73	4.44	2.67
K_2O	1.82	2.77	0.86	1.23	1.85	0.84	1.27	2.75	3.72	1.72	0.92	0.84	0.67
P_2O_5	0.37	0.34	0.24	0.24	0.24	0.26	0.24	0.2	0.2	0.26	0.25	0.32	0.34
LOI	2.58	2.17	4.01	3.91	5.54	5.45	4.97	4.56	4.79	3.84	6.78	1.28	2.88
Mg#	59	52	77	77	79	80	81	68	63	68	54	55.41	64.47
La	3.69	8.28	2.80	4.59	3.61	3.73	5.56	4.03	3.85	6.75	8.11	12.5	14
Ce	7.75	15.4	6.89	10	7.53	8.17	10.68	11	10.9	15.1	13.9	21.6	26.1
Pr	1.15	2.34	1.08	1.37	1.16	1.27	1.49	1.77	1.82	2.14	2.04	3.42	4.18
Nd	5.48	12.3	5.34	6.22	5.39	6.15	6.51	9.38	9.91	9.78	10	15	19.2
Sm	1.60	3.51	1.73	1.80	1.55	1.77	1.72	3.02	3.27	2.8	2.65	3.86	4.7
Eu	0.55	1.14	0.60	0.58	0.47	0.52	0.46	1.06	1.15	0.88	0.92	1.35	1.61
Gd	1.87	3.53	2.02	1.93	1.64	1.94	1.74	3.70	4.19	2.94	2.54	4.07	4.93
Tb	0.33	0.68	0.33	0.33	0.29	0.34	0.31	0.62	0.68	0.51	0.45	0.74	0.89
Dy	2.07	4.60	2.18	2.13	1.90	2.19	1.95	3.99	4.39	3.17	3.16	5.11	6.18
Ho	0.44	0.89	0.44	0.43	0.4	0.46	0.39	0.8	0.91	0.65	0.67	1.07	1.27
Er	1.24	2.68	1.29	1.24	1.16	1.31	1.12	2.31	2.56	1.92	1.88	2.98	3.38
Tm	0.20	0.42	0.19	0.18	0.18	0.20	0.18	0.32	0.35	0.28	0.24	0.4	0.44
Yb	1.28	2.63	1.22	1.21	1.19	1.30	1.18	2.01	2.18	1.88	1.43	2.24	2.62
Lu	0.19	0.34	0.18	0.17	0.19	0.20	0.19	0.29	0.30	0.29	0.21	0.35	0.41
Ba	201	858	162	199	305	161	204	1355	2735	260	655	205	183
Cu	94.8		9.0	48.3	64.5	128.9	148.3	109.0	124.0	90.1			
Sr	295	440	232	350	145	188	164	894	1180	300	348	394	449
V	227	570	213	188	202	219	185	208	249	210	802	248	251
Zn	56.6		74.6	72.7	58.3	65.7	60.0	79.4	78.7	80.2			
Co	35.5	39.5	53.2	52.3	64.3	60.9	64.4	44.0	40.2	34.8	26.9	28.7	37.5
Ga	9.8	26.0	12.6	12.5	8.4	9.7	7.6	16.5	20.7	15.0	29.6	30.9	30.8
Pb	2.71		6.15	6.42	2.55	2.49	2.12	6.44	4.56	3.26			
Rb	13.3	44.0	14.3	17.5	18.6	11.9	15.3	41.5	73.5	30.3	15.6	19.8	11.0
Sc	41.6		38.2	38.3	34.1	40.9	33.7	30.4	38.1	31.4			
Th	0.51		0.30	0.71	0.71	0.69	0.72	0.28	0.24	0.86		1.75	3.26
U	0.306	1.46	0.20	0.43	0.28	0.32	0.31	0.30	0.12	0.46	0.80	0.80	0.92
Cr	366	111	888	946	717	670	1041	622	259	444	9	93	168
Ni	91	29	283	29	3079	2549	4539	156	86	91	15	40	110
Zr	29.2	106.0	24.6	25.8	25.4	27.4	25.8	56.1	58.1	65.0	91.1	129.0	172.0
Nb	2.11	3.73	1.05	0.97	1.51	1.75	1.57	1.21	0.88	2.08	3.51	6.50	8.60
Hf	0.92	4.74	0.77	0.79	0.728	0.86	0.738	1.75	1.72	1.64	3.13	4.06	4.56
Ta	0.114	<0.5	0.07	0.1	0.084	0.087	0.078	0.120	0.10	0.25	<0.5	0.650	1.020
Y	11.33	19.50	9.94	9.10	9.99	10.50	9.92	20.10	21.20	17.60	12.70	20.60	25.30
Reference	This study												

Sample	348yQ-68	348yQ-71	JZL04-5	JZL04-7	yQ-30	yQ-31	yQ-32	ZHB04-2	ZHB04-9	ZHB04-10	ZHB04-11	Z19-2
Rock	B	B	B	BA	B	B	B	A	B	B	B	A
Formation	Yundukala	Jiangzierkuduke			Nanmingshui			Batamayineishan				
SiO_2	52.96	48.27	52.56	56.03	47.02	48.02	47.26	56.98	48.44	52.99	51.74	56.83
TiO_2	0.69	3.01	1.90	1.43	1.82	2.19	1.74	1.46	2.26	2.16	1.75	1.77
Al_2O_3	18.27	14.48	15.83	15.27	15.31	14.55	15.31	15.17	16.31	16.42	16.58	15.68
Fe_2O_3	1.38	2.19	4.14	2.60	1.63	1.68	1.61	5.55	8.31	6.68	6.71	5.50
FeO	6.88	10.93	5.05	4.52	10.88	11.23	10.71	2.17	2.41	3.25	3.02	2.88
MnO	0.25	0.22	0.16	0.13	0.21	0.20	0.16	0.08	0.15	0.12	0.14	0.15
MgO	3.17	4.45	4.21	3.57	8.30	7.84	7.47	3.57	3.49	3.19	5.00	3.07
CaO	8.69	7.14	6.53	4.89	9.97	9.16	10.30	4.12	7.48	7.42	4.76	7.71
Na_2O	3.21	3.31	4.02	4.03	2.58	3.12	3.25	4.40	3.94	3.52	4.81	3.12
K2O	1.70	1.06	1.92	2.92	0.19	0.22	0.36	2.20	1.16	0.75	2.44	0.81
P_2O_5	0.25	1.33	0.74	0.54	0.22	0.32	0.22	0.66	0.93	0.64	0.47	0.77
LOI	2.54	3.58	2.95	4.06	1.87	1.48	1.62	3.65	5.13	2.87	2.58	1.69

Please cite this article as: Zhang, Z., et al., Late Paleozoic volcanic record of the Eastern Junggar terrane, Xinjiang, Northwestern China: Major and trace element characteristics, Sr–Nd isotopic systematics and implications ..., Gondwana Research (2009), doi:10.1016/j.gr.2009.03.004

Table 1 (*continued*)

Sample	348yQ-68	348yQ-71	JZL04-5	JZL04-7	yQ-30	yQ-31	yQ-32	ZHB04-2	ZHB04-9	ZHB04-10	ZHB04-11	Z19-2
Rock	B	B	B	BA	B	B	B	A	B	B	B	A
Formation	Yundukala	Jiangzierkuduke			Nanmingshui			Batamayineishan				
Mg#	45.49	42.46	50.65	52.72	59.00	56.83	56.81	51.63	43.00	42.42	54.12	45.64
La	12.60	34.50	36.60	42.70	9.35	13.3	8.96	41.23	45.85	19.71	23.89	24.96
Ce	19.60	63.60	76.90	82.50	19.90	28.40	19.20	79.23	96.07	42.42	50.57	56.25
Pr	2.78	9.22	9.96	10.6	3.75	4.63	3.29	10.04	11.59	6.61	7.03	8.01
Nd	12.60	46.50	41.90	41.70	15.70	22.40	15.20	40.56	47.92	29.35	29.96	35.05
Sm	3.18	10.50	8.53	8.32	4.21	5.88	4.24	8.08	9.93	6.98	6.95	7.13
Eu	1.06	3.09	2.67	1.99	1.53	1.92	1.64	2.11	2.77	2.27	2.20	2.26
Gd	3.34	9.88	8.25	7.39	4.89	6.62	4.77	6.56	8.43	6.99	6.88	6.64
Tb	0.62	1.59	1.30	1.19	0.88	1.19	0.85	1.08	1.40	1.13	1.13	1.03
Dy	4.59	10.2	7.28	6.92	6.15	7.75	5.86	5.87	7.26	6.72	6.63	5.98
Ho	0.91	1.94	1.54	1.47	1.22	1.47	1.11	1.23	1.51	1.42	1.43	1.18
Er	2.87	5.36	4.15	3.85	3.42	4.02	3.18	3.35	4.04	3.84	3.77	3.36
Tm	0.40	0.66	0.66	0.61	0.47	0.57	0.42	0.49	0.58	0.57	0.60	0.47
Yb	2.36	4.05	4.19	4.15	2.74	3.15	2.32	3.32	3.91	3.85	4.05	3.03
Lu	0.38	0.61	0.64	0.55	0.35	0.43	0.28	0.51	0.55	0.54	0.54	0.45
Ba	551	403	622.3	408.5	60.3	49	24.9	577.55	443.79	351.02	600.91	309
Cu			21.76	27.46				90.43	57.94	57.36	31.7	
Sr	308	654	569.5	509.1	232	278	334	358	644	496	608	530
V	191	292			366	385	350					
Zn			99.15	85.78				84.47	105.88	93.42	101.17	
Co	21.6	31.2	24.8	21.0	46.6	38.1	41.0	20.3	29.6	50.1	38.4	10.0
Ga	30.5	33.0	17.7	17.0				15.0	17.5	16.0	18.2	
Pb			6.11	8.78				9.21	7.32	4.39	4.86	
Rb	23.6	23.7	19.3	48.4	4.9	5.1	13	25.3	9.1	10.8	36.4	
Sc			20.4	15.3				18.6	22.7	24.0	23.7	30.4
Th	1.69	4.30	2.58	4.87	3.08	3.40	2.09	2.45	1.64	1.41	2.08	
U	0.92	0.92	1.14	2.11	0.92	0.80	0.80	1.05	0.68	0.42	0.82	
Cr	18.6	8.6	50.8	63.8	234.0	209.0	236.0	103.1	100.4	133.7	137.8	67.0
Ni	22.2	12.2	18.9	28.0	121.0	91.5	104.0	53.1	70.0	97.6	96.4	118.0
Zr	143.0	210.0	352.9	282.2	121.0	176.0	147.0	284.8	285.7	209.4	251.6	209.0
Nb	6.2	13.8	17.1	19.0	6.2	8.7	4.5	17.7	21.0	7.9	11.1	16.7
Hf	3.79	5.96	7.33	6.56	3.65	5.01	4.59	5.95	6.43	4.68	5.52	
Ta	0.50	1.85	1.07	1.34	0.38	0.63	0.29	0.85	1.12	0.56	0.74	
Y	18.80	40.60	35.25	32.36	25.20	30.30	22.60	30.29	35.33	31.50	32.59	30.37
Reference	This study											Mei et al. (1993)

The major element data are in wt.%, and trace element data are in ppm. The analyses are recalculated to 100% volatile-free. Mg# = molar Mg/(Mg + Fe) × 100; P = picrite; BA = basaltic andesite; ANK = ankaramite; B = basalt; A = andesite; D = dacite. The blank represents the concentrations which have not been determined.

address the source of the magmas. We used here different t values for age-correction: 400 Ma, 385 Ma, 340 Ma and 310 Ma are used for the Tuoranggekuduke, Beitashan, Nanmingshui and Batamayineishan Formations respectively. As a whole, all Paleozoic volcanic rocks in the study area have relatively homogeneous isotopic Sr and Nd compositions (Table 2), which are characterized by low $(^{87}Sr/^{86}Sr)_t$

Table 2
Sr and Nd isotopic data of the volcanic rocks from the Eastern Junggar terrane.

Sample	Formation	Rb (ppm)	Sr (ppm)	$^{87}Rb/^{86}Sr$	$^{87}Sr/^{86}Sr$	$(^{87}Sr/^{86}Sr)_t$	Sm (ppm)	Nd (ppm)	$^{147}Sm/^{144}Nd$	$^{143}Nd/^{144}Nd$	$(^{143}Nd/^{144}Nd)_t$	$\varepsilon_{Nd}(t)$	Reference
A0322	Tuoranggekeuduke			0.05184	0.705177	0.704888			0.127561	0.512676	0.512342	4.27	Zhang et al. (2004)
A0623				0.093448	0.705154	0.704633			0.128005	0.512624	0.512289	3.24	
A1022				0.05381	0.705079	0.704779			0.126503	0.512644	0.512313	3.70	
A0422				0.091775	0.704435	0.703923			0.126393	0.512713	0.512382	5.06	
A0521				0.111976	0.704519	0.703895			0.124643	0.51273	0.512404	5.48	
XJ20-6	Beitashan	18.97	154.0	0.3564	0.705467	0.703555	1.498	5.511	0.1643	0.512920	0.512506	7.10	This study
XJ21-20		2.129	123.8	0.0497	0.704437	0.704170	1.648	5.233	0.1903	0.512976	0.5124966	6.91	
XJ21-22		1.321	51.47	0.0743	0.704586	0.704187	1.847	6.454	0.1730	0.512930	0.5124935	6.86	
XJ22-8		4.781	740.5	0.0187	0.704060	0.703960	2.976	13.16	0.1367	0.512839	0.5124949	6.89	
XJ22-10		17.34	225.5	0.2225	0.705273	0.704079	1.439	4.594	0.1894	0.512995	0.5125170	7.32	
XJ22-12		13.23	304.2	0.1257	0.705001	0.704326	1.514	5.072	0.1804	0.512943	0.5124880	6.75	
XJ23-14		11.55	210.9	0.1584	0.704602	0.703752	1.811	6.257	0.1750	0.512942	0.5125012	7.01	
XJ23-17		1.883	54.92	0.0992	0.703809	0.703277	0.7892	1.982	0.2407	0.513078	0.5124713	6.43	
XJ23-17-1		13.85	182.0	0.2201	0.705124	0.703943	1.733	6.646	0.1577	0.512888	0.5124910	6.81	
YQ-30	Nanmingshui						4.03	14.01	0.1740	0.512985	0.512598	7.76	
YQ-31							5.74	21.06	0.1649	0.512979	0.512612	8.04	
YQ-32							4.10	14.01	0.1769	0.513014	0.51262	8.20	
ZHB-12	Batamayineishan	3.20	364	0.0252	0.705534	0.70542	2.03	6.87	0.1788	0.512989	0.512634	7.6	Long et al. (2006)
ZHB-15		3.77	343	0.0317	0.705426	0.70528	2.56	7.71	0.2012	0.513028	0.512606	7.4	
ZHB-17		3.32	393	0.0245	0.705448	0.70534	2.50	8.95	0.1690	0.512931	0.512577	6.9	
ZHB-20		3.45	216	0.0458	0.705559	0.70535	2.32	7.81	0.1798	0.512954	0.512577	6.9	
ZHB-22		7.22	166	0.1254	0.705880	0.70531	2.56	8.63	0.1793	0.512939	0.512563	6.6	
ZHB-24		2.95	312	0.0272	0.705462	0.70534	2.37	7.96	0.1803	0.512958	0.512580	6.9	

400 Ma, 385 Ma, 340 Ma and 310 Ma for age correction are used for the Tuoranggekuduke, Beitashan, Nanmingshui and Batamayineishan Formations respectively.

Please cite this article as: Zhang, Z., et al., Late Paleozoic volcanic record of the Eastern Junggar terrane, Xinjiang, Northwestern China: Major and trace element characteristics, Sr–Nd isotopic systematics and implications ..., Gondwana Research (2009), doi:10.1016/j.gr.2009.03.004

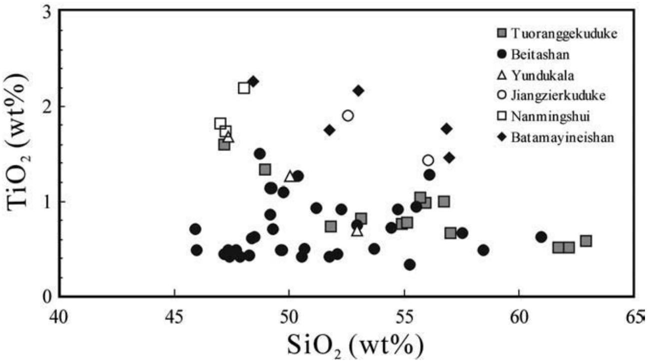

Fig. 2. TiO_2 versus SiO_2 diagram of the Paleozoic volcanic rocks in the Eastern Junggar terrane.

ratios (0.7033–0.7054) and positive $\varepsilon_{Nd}(t)$ values (+3.2 to +8.2). The samples from the NS Fm. have the highest $\varepsilon_{Nd}(t)$ values (~+8), whereas those from the BN Fm. have the highest $(^{87}Sr/^{86}Sr)_t$ ratios (~0.7053). The samples from the TK and BS Fms. exhibit similar $(^{87}Sr/^{86}Sr)_t$ ratios (0.7033–0.7049), but those from the BS Fm. have much higher $\varepsilon_{Nd}(t)$ values (+6.4 to +7.3) than the latter (+3.7 to +5.5). Similarly, those from the BS and BN Fms. have similar $\varepsilon_{Nd}(t)$ values (+6.4 to +7.6), but the samples from the BN Fm. have much higher $(^{87}Sr/^{86}Sr)_t$ ratios (Table 2). Interestingly, all Paleozoic igneous rocks in the Junggar terrane, including both extrusive and intrusive rocks, mafic–ultramafic and felsic rocks, display low $(^{87}Sr/^{86}Sr)_t$ ratios (<0.706) and positive $\varepsilon_{Nd}(t)$ values (Wu et al., 2000; Hong et al., 2003a; Zhang et al., 2008b). Obviously, except for the BN Fm., the volcanic rocks from the Eastern Junggar terrane are isotopically distinct from those commonly observed in continental basalts (e.g., Hawkesworth et al., 1984; Carlson and Hart, 1988; Fedorenko and Doherty, 1993; Wooden et al., 1993), but similar to oceanic basalts (e.g., Mahoney, 1988; Ellam and Cox, 1989; Carlson, 1991; Hergt et al., 1991).

6. Discussion

6.1. Volcanic series

Confirming which volcanic rock series a group of flows belongs to is very important to help discriminate the tectonic setting of the volcanic rocks. With one exception (H-11), all Nb/Y ratios are below 0.7, implying that the rocks are subalkaline (Winchester and Floyd, 1977). When plotted on a FeO* versus FeO*/MgO diagram (Miyashiro, 1975), the basalts from the NS Fm. all lie in the tholeiite field, while those from the YK Fm. fall in the calc-alkaline field (Fig. 4). In contrast, the volcanic rocks from other Fms. fall in both the tholeiite and calc-

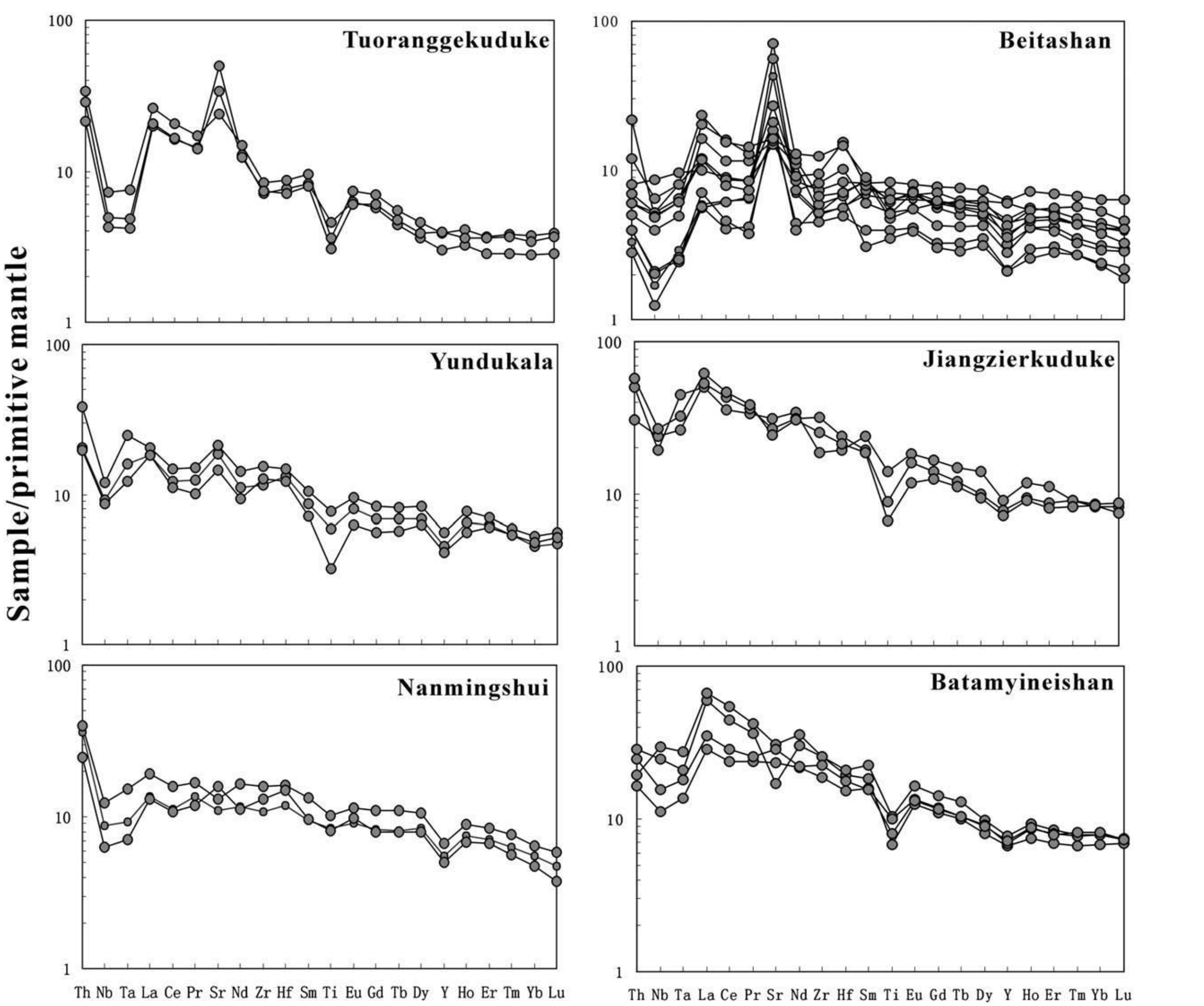

Fig. 3. Primitive mantle-normalized trace element patterns of the Paleozoic volcanic rocks in the Eastern Junggar terrane. Normalized values are from Sun and McDonough (1989).

Please cite this article as: Zhang, Z., et al., Late Paleozoic volcanic record of the Eastern Junggar terrane, Xinjiang, Northwestern China: Major and trace element characteristics, Sr–Nd isotopic systematics and implications ..., Gondwana Research (2009), doi:10.1016/j.gr.2009.03.004

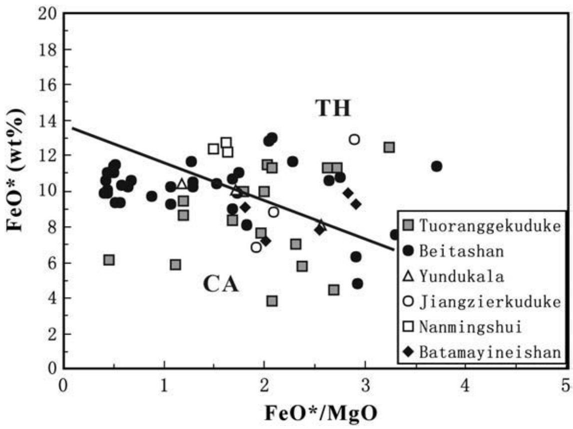

Fig. 4. FeO* versus FeO*/MgO diagram of the Paleozoic volcanic rocks in the Eastern Junggar terrane (after Miyashiro, 1975).

alkaline fields, but most samples from the BN Fm. plot in the tholeiite field (Fig. 4).

6.2. Implications for the tectonic evolution of the Eastern Junggar terrane during the Late Paleozoic

The tectonic evolution of the Eastern Junggar terrane during the Late Paleozoic is still debated. Considerable controversy surrounds three issues: 1) the tectonic setting of the Devonian volcanic rocks, i.e., island arc (e.g., Yu et al., 1993; He et al., 1994; Windley et al., 2002), active continental margin (Mei et al., 1993; Chen and Jahn, 2002), or rift (Han, 1991; Wei and Ni, 1990) or mantle plume (Wang et al., 2002)?; 2) If the Devonian volcanic rocks formed in an island arc, are they related to northward subduction of the Junggar ocean (Hong et al., 2003b) or southward subduction of Paleo-Asian ocean (Xu et al., 2001; Zhang et al., 2004)?; 3) When did the collision between Siberian plate and Kazakhstan block occur, Early Carboniferous, Late Carboniferous or Permian? Cocks and Torsvik (2007) point out that the entire Junggar terrane was unified by the latest Carboniferous on the basis of a large paleontological and paleomagnetic and literature database, and they point out that the Tarim, Central Tianshan and Junggar terranes had all amalgamated by at least the latest Carboniferous. The Tarim–Junggar–Tianshan aggregated terranes did not combine with the Siberian craton until the Early Permian. Tarim became welded to Siberia during the Mid-Permian. Siberia appears to have started to collide with the “Kazakhstania Terrane Assemblage” during the Early Permian. Xiao et al. (2008) proposed that the formation of a complicated orogenic collage between the Siberian and Tarim cratons occurred/continued between the end-Permian and Triassic. In contrast, Li et al. (2003) proposed that the collision between the two cratons occurred in the Late Early Carboniferous in the Junggar, but in the Late Carboniferous in Tianshan, whereas Buslov et al. (2004) suggested that the Kazakhstan block collided with Siberian craton during Late Carboniferous to Permian.

Here, we use geochemical data to constrain the tectonic settings of the Paleozoic volcanic rocks in the Eastern Junggar terrane, and then discuss their tectonic evolution during the Late Paleozoic.

6.2.1. Tuoranggekuduke Formation

The Early Devonian Tuoranggekuduke Fm. consists of a suite of tholeiite to calc-alkaline basalt, andesite, dacite and rhyolite. The lavas exhibit a significant trough at Nb, Ta and Ti on the primitive mantle-normalized trace element patterns (Fig. 3), a typical characteristic of subduction-related magmas. The basaltic rocks fall in the volcanic arc field when plotted on a 2Nb–Zr/4–Y diagram (Fig. 5). In addition, the dacites show many geochemical similarities to adakites, e.g., high Sr contents (560–757 ppm, >400 ppm), relatively high Ni contents (39–97 ppm, >24 ppm) and low Y (<18 ppm) and Yb contents (<1.8 ppm), FeO + MgO + TiO_2 contents (6.3–9.1), consistent with the characteristics of adakites (Defant and Drummond, 1990; Drummond and Defant, 1990; Martin, 1999). It is generally considered that adakites are derived from very low degrees of melting of subducted oceanic crust in an island arc setting during the early stage of subduction (Schiano et al., 1995). Therefore, it is very likely that the volcanic rocks from the TK Fm. formed in an island arc setting, probably an immature volcanic arc, as indicated by the presence of adakites.

6.2.2. Beitashan Formation

The Middle Devonian Beitashan Fm. comprises dominantly tholeiite to calc-alkaline basic to intermediate rocks (Fig. 4). They are also geochemically characterized by remarkably negative Nb and Ti anomalies on the trace element patterns (Fig. 3). The picrites, ankaramites and basalts, which have been considered to be evolved from a common parental high-Mg basaltic magma (Zhang et al., 2008b), have subchondritic Nb/Ta ratios (<17), indicating the derivation from a mantle source metasomatized by slab-derived fluids (Ben Othman et al., 1989). Additionally, the picrites, ankaramites and basalts have similar Zr/Nb and Sm/Nd ratios to MORBs, which show values for these two ratios between 10–60 (Davidson, 1996) and ~0.32 (Andersen, 1997). Hence, the volcanic rocks have similar HFSE ratios to MORBs. Combined with the negative Nb and Ti anomalies coupled with high $\varepsilon_{Nd}(t)$ values (6.4–7.3), it can be inferred that the volcanic rocks from the BS Fm. also formed in an island arc setting.

6.2.3. Yundukala Formation

The basalts from the Middle Devonian YK Fm. have geochemical similarities to basalts from the BS Fm., i.e., remarkably negative Nb and Ti anomalies on the trace element patterns coupled with subchondritic Nb/Ta ratios (<17) and similar Zr/Nb (10–23) and Sm/Nd ratios (24–26) to MORBs. The lavas also lie in the volcanic arc field in the 2Nb–Zr/4–Y diagram (Fig. 5). Consequently, like the BS Fm., the YK Fm. may also have formed in an island arc setting.

6.2.4. Jiangzierkuduke Formation

The Late Devonian JK Fm. consists dominantly of a suite of calc-alkaline intermediate-basic to intermediate-acid rocks. The intermediate-basic rocks also display troughs at Nb and Ti on the primitive mantle-normalized trace element patterns (Fig. 3). When plotted on

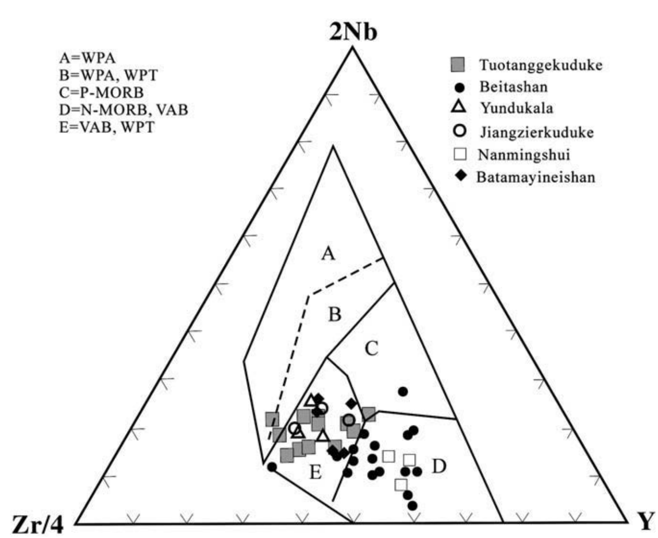

Fig. 5. 2Nb–Zr/4–Y diagram of the Paleozoic volcanic rocks in the Eastern Junggar terrane (after Meschede, 1986).

Please cite this article as: Zhang, Z., et al., Late Paleozoic volcanic record of the Eastern Junggar terrane, Xinjiang, Northwestern China: Major and trace element characteristics, Sr–Nd isotopic systematics and implications ..., Gondwana Research (2009), doi:10.1016/j.gr.2009.03.004

the 2Nb–Zr/4–Y diagram (Fig. 5), they also fall in the volcanic arc field. Therefore, we propose that they formed in an island arc setting. However, unlike those from the BS and YK. Fms., the volcanic rocks from the JK Fm. have higher incompatible element concentrations and more enrichment of highly incompatible element concentration relative to moderately incompatible elements (Table 1, Fig. 3). Furthermore, they have higher TiO_2 contents (1.4–3.0%). Given the fact that the JK Fm. contains a large amount of tuff and sandstone and that the volcanic rocks have dominant calc-alkaline affinities, we propose that the Formation formed in a mature island arc setting.

6.2.5. Nanmingshui Formation

Unlike other formations, the Early Carboniferous NS Fm. consists of tholeiitic basalts. Although they also exhibit negative Nb, Ta and Ti anomalies on the primitive mantle-normalized trace element patterns (Fig. 3), there is no significant enrichment of highly incompatible elements relative to moderately incompatible ones, and low $(La/Yb)n$ ratios (2.3–2.8). In addition, they have higher TiO_2 contents (1.7–2.2 wt.%), close to MORB. Furthermore, their $\varepsilon_{Nd}(t)$ values (~+8) are slightly lower than those of MORBs (~+10), and the samples plot in the N-MORB and VAB field in the 2Nb–Zr/4–Y diagram (Fig. 5). Hence, the basalts from the NS Fm. display a transitional feature between island arc and mid-ocean ridge basalts. In general, back-arc basalts have geochemical signatures between N-MORB and island arcs (Hollings and Kerrich, 2004). For instance, back-arc basin mafic volcanic rocks in the Sumisu area, middle Izu arc (Hochstaedter et al., 1990a,b), are slightly depleted in HFSE and REE, with high positive $\varepsilon_{Nd}(t)$ values ranging from 6.2 to 9.4. These rocks have compositions similar to the volcanic rocks from the NS Fm. Interestingly, Xu et al. (2001) also recognized an Early Carboniferous back-arc volcanic assemblage at the Kuerti region, which is located in the western part of the Eastern Junggar terrane.

6.2.6. Batamayineishan Formation

The Late Carboniferous BN Fm. is composed of a succession of tholeiitic to calc-alkaline continental basic-intermediate volcanic rocks. Although they exhibit negative Ti anomalies, they have no significantly negative Nb or Ta anomalies like those from other formations, and they have higher absolute TiO_2 contents (1.5–2.3 wt.%). Additionally, they have high incompatible element concentrations and more enrichment of highly incompatible elements relative to moderately incompatible ones as well as high $(^{87}Sr/^{86}Sr)_t$ ratios (~0.705). When plotted in a 2Nb–Zr/4–Y diagram (Fig. 5), they lie in the within plate basalt and volcanic arc basalt field. On the Th/Yb versus Ta/Yb and Zr/Y versus Zr diagrams (Fig. 6), all samples plot in the within plate basalt field. In addition, as stated above, the volcanic rocks from the BN Fm. formed in a continental setting as many researchers proposed (e.g., Yang et al., 2001; Zhu et al., 2005; Long et al., 2005). Thus, we suggest that the BN Fm. formed within a continental plate, which is consistent with Yang et al. (2001) and Zhu et al.'s (2005) conclusions. Interestingly, some other researchers also regarded the volcanic rocks of Carboniferous–Permian age in the Chinese Tianshan as due to post-collisional intraplate extension characterized by continental rifting (Che et al., 1996; Xia et al., 2004; Liu et al., 2006; de Jong et al., 2008; Wang et al., 2009). Xu et al. (2006) regarded Carboniferous granites as post-collisional. Carboniferous basic lavas dominate (>80 vol.%) the Tianshan Carboniferous–Permian rift system. Similarly, Sun et al. (2008) proposed that the western Tianshan orogen experienced a transformation from convergence to extension in the Late Carboniferous based on the geochemical characteristics of the volcanic rocks in the southern Awulala mountains. Using zircon U–Pb LA-ICPMS ages and geochemical data from igneous rocks of the western Tianshan, Wang et al. (2009) argued that the igneous activity from Carboniferous to Permian time evolved from calc-alkaline to alkaline. The association of high-K calc-alkaline, transitional and alkaline granites of Early to Middle Permian age suggests a post-collisional setting. This point to a transition from Carboniferous convergence to a Permian anorogenic intraplate environment. Early–Middle Permian plutons are associated with dextral strike-slip faults. In addition, Wang et al. (2009) proposed that post-collisional lithosphere-scale transcurrent shear zones controlled the magmatic activity during the transition from a convergent margin to an anorogenic intraplate setting. de Jong et al. (2008) proposed that this occurred in a non-plume-related Yellowstone-like extensional–transtensional tectonic regime.

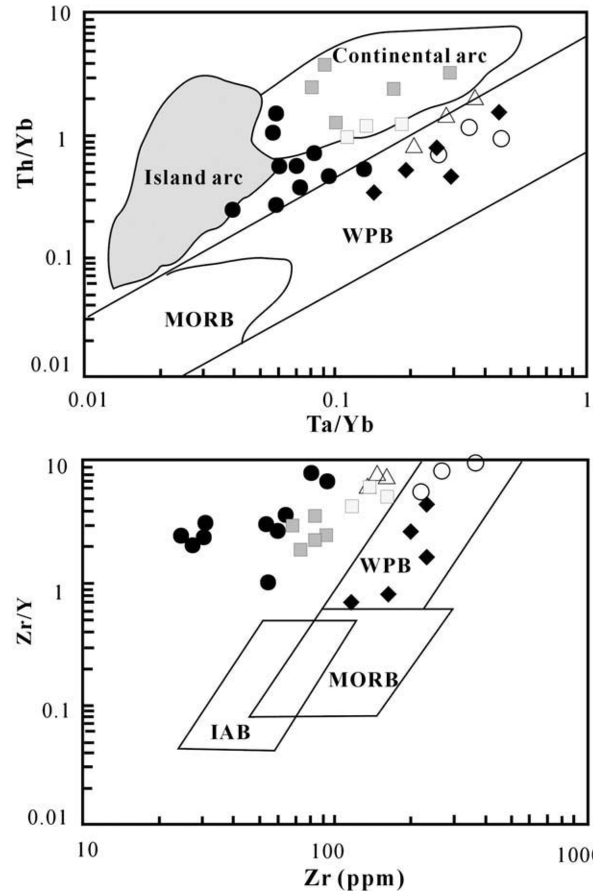

Fig. 6. Th/Yb versus Ta/Yb and Zr/Y versus Zr diagrams of the Paleozoic volcanic rocks in the Eastern Junggar terrane (after Pearce and Norry, 1979). The symbols are the same as Fig. 5.

6.3. Tectonic evolution

As discussed above, we propose that the Early Devonian Tuoranggekuduke Formation, Middle Devonian Beitashan Formation and Middle Devonian Yundukala Formation formed in island arc environment, possible an immature volcanic arc, and the Late Devonian Jiangzierkuduke Formation likely formed in a mature island arc setting as indicated by increasing TiO_2. In contrast, the Early Carboniferous Nanmingshui Formation probably formed in a back-arc environment, and the Late Carboniferous Batamayineishan Formation may have formed within a continental plate. Thus, it can be inferred that the study area experienced a range in conditions, changing from an immature island arc in Early Devonian to a mature island arc in Late Devonian, and then to back-arc spreading in Early Carboniferous. However, the preserved continental intraplate volcanic rocks of the BN Fm. suggest that the collision between Siberian plate (Altai terrane) and Kazakhstan block (Junggar terrane) should have occurred before the BN Fm. formed, i.e., at the end of Early Carboniferous to the Middle–Late Carboniferous (ca. 309 Ma). This conclusion is compatible with the recently reported Re–Os isotopic and SHRIMP U–Pb zircon ages (282.5 ± 4.8 Ma, 290.2 ± 6.9 Ma; 287 ± 5 Ma) of the Cu–Ni sulfide ores and hosted mafic intrusions in the Kalatongke area, which

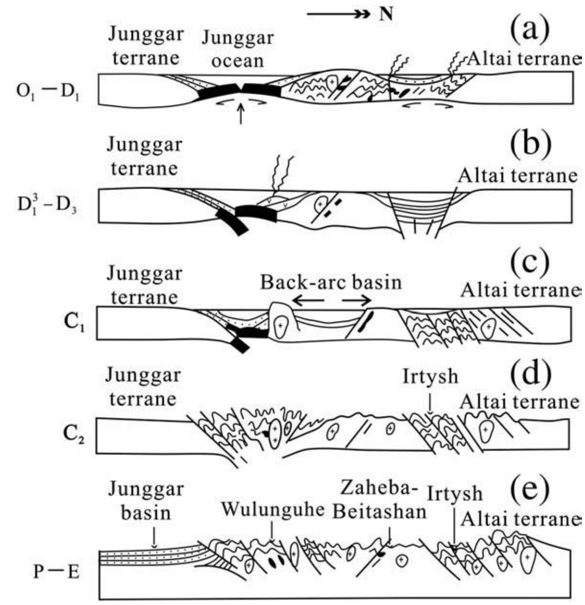

Fig. 7. Schematic cross-sections showing the tectonic evolution of the Eastern Junggar terrane in the Late Paleozoic. See text for detailed interpretation.

was formed in a post-collisional extensional continental intraplate setting (Han et al., 2004; Zhang et al., 2008a; Pirajno et al., 2008), although some workers argued that these mafic–ultramafic intrusions were emplaced in a subduction-related setting (e.g., Xiao et al., 2008).

Regionally, the 481–489 Ma Wulunguhe ophiolite belt has been identified on the south side of the Late Paleozoic volcanic rocks in the Eastern Junggar terrane, and the ophiolite has been considered to represent the ancient oceanic crust of the Junggar ocean (Jian et al., 2003; Deng and Wang, 1995). In addition, the NS Fm. formed in a back-arc basin is situated on the northernmost side of the ophiolite belt. Hence, it can be inferred that the formation of the Late Paleozoic arc-related volcanic rocks in the study area could be related to northward subduction of the ancient Junggar ocean.

In combination with the previous geochronological data and our new geochemical data, we propose a model that involves a volcanic arc formed by northward subduction and amalgamation of different terranes during the Late Paleozoic (Fig. 7). In this model, the ancient Junggar ocean separated the Junggar terrane and Altai terrane from Early Ordovician to Early Devonian (Fig. 7a). Northward subduction created an arc along the southern margin of the Altai terrane, where the volcanic rocks of the TK Fm. formed at 408 Ma (Fig. 7b). Partial melting of subducted oceanic rocks in an arc setting produced silicic magmas that formed the TK felsic volcanic rocks, whereas partial melting of the mantle wedge resulted in the formation of the TK mafic magmas. Continued northward subduction gave rise to produce the BS, YK and JK volcanic rocks (Windley et al., 2002), and eventually resulted in back-arc spreading and the formation of a back-arc basin (Fig. 7c). Collision of the Junggar and Altai terranes resulted in their final amalgamation into a Cordilleran-type orogen (Goldfarb et al., 2003) at the end of the Early Carboniferous to the Middle–Late Carboniferous (Fig. 7d). The BN volcanic rocks formed in an extensional setting following the collision. From the Permian until ca. 55–50 Ma (Tertiary), the Junggar terrane remained a tectonically stable region with little significant relief (Fig. 7e). However, the collision of India with Asia, just after the start of the Tertiary, initiated a more recent period of extreme uplift (Goldfarb et al., 2003; Zhang et al., 2008c).

7. Conclusions

The Late Paleozoic volcanic rocks in the Eastern Junggar terrane consist of a series of Early Devonian to Early Carboniferous marine subduction-related mafic to felsic rocks and Late Carboniferous continental mafic rocks. The Early Devonian Tuoranggekuduke Formation, Middle Devonian Beitashan Formation and Middle Devonian Yundukala Formation formed in island arc environment, possible an immature volcanic arc, and the Late Devonian Jiangzierkuduke Formation likely formed in a mature island arc setting. The Early Carboniferous Nanmingshui Formation formed in a back-arc environment. These Early Devonian to Early Carboniferous subduction-related volcanic rocks were formed as a result of the northward subduction of the ancient Junggar ocean. In contrast, the Late Carboniferous Batamayineishan Formation formed in a continental intraplate setting. The terranes of the Altai and Junggar regions were fully amalgamated into a Cordilleran-type orogen by the end of Early Carboniferous to the Middle–Late Carboniferous.

Acknowledgements

Constructive reviews and suggestions by Dr. Koen de Jong and an anonymous reviewer helped to improve the revised version. This material is based upon work supported by NSFC grant (40772045, 40572047), National 305 Project (2007BAB25B05), the 111 Project (B07011) and PCSIRT. We are thankful for constructive suggestions by Profs. Li Jingyi and Han Baofu.

References

Andersen, T., 1997. Radiogenic isotope systematics of the Herefoss granite, South Norway: an indicator of Sveconorwegian (Grenvillian) crustal evolution in the Baltic Shield. Chemical Geology 135, 139–158.
Barnes, S.J., Naldrett, A.J., Gorton, M.P., 1985. The origin of the fractionation of platinum-group elements in terrestrial magmas. Chemical Geology 53, 303–323.
Ben Othman, D., White, W.M., Patchett, J., 1989. The geochemistry of marine sediments, island arc magma genesis, and crust–mantle recycling. Earth and Planetary Science Letters 94, 1–21.
Beswick, A.E., 1982. Some geochemical aspects of alteration and genetic relations in komatiitic suites. In: Arndt, N.T., Nisbet, E.G. (Eds.), Komatiites. George Allen and Unwin, London, pp. 283–308.
Briggs, S.M., Yin, A., Manning, C.E., Chen, Z.L., Wang, X.F., Grove, M., 2007. Late Paleozoic tectonic history of the Ertix Fault in the Chinese Altai and its implications for the development of the Central Asian Orogenic System. Geological Society of America Bulletin 119, 944–960.
Buckman, S., Aitchison, J.C., 2004. Tectonic evolution of Paleozoic terranes in West Junggar, Xinjing, NW China. In: Malpas, J., Fletcher, C.J.N., Ali, J.R., Aitchison, J.C. (Eds.), Aspects of the Tectonic Evolution of China. Geol Soc Lond Spec Publ, vol. 226, pp. 101–129.
Buckman, S., Aitchison, J.C., 2001. Middle Ordovician (Llandeilan) radiolarians from West Junggar, Xinjiang, China. Micropaleontology 47, 359–367.
Buslov, M.M., Fujiwara, Y., Iwata, K., Semakov, N.N., 2004. Late Paleozoic–Early Mesozoic geodynamics of Central Asia. Gondwana Research 7, 791–808.
Carlson, R.W., 1991. Physical and chemical evidence on the cause and source characteristics of flood basalt volcanism. Austrial Journal of Earth Sciences 38, 525–544.
Carlson, R.W., Hart, W.K., 1988. Flood basalt volcanism in the northwestern United States. In: Macdougall, J.D. (Ed.), Continental Flood Basalts. Kluwer Academic Publishers, Dordrecht, pp. 35–62.
Charvet, J., Shu, S.L., Laurent-Charvet, S., 2007. Paleozoic structural and geodynamic evolution of eastern Tianshan (NW China): welding of the Tarim and Junggar plates. Episodes 30, 162–186.
Chai, F., Mao, J., Dong, L., Yang, F., Liu, F., Geng, X., Zhang, Z., 2009-this issue. Geochronology of metarhyolites from the Kangbutiebao formation in the Kelang basin, Altay Mountains, Xinjiang: implications for the tectonic evolution and metallogeny. Gondwana Research.
Che, Z.C., Liu, L., Liu, H.F., Luo, J.H., 1996. Review on the ancient Yili rift, Xinjiang, China. Acta Petrol Sin 12, 478–490 (in Chinese with English abstract).
Chen, B., Jahn, B.M., 2004. Genesis of post-collisional granitoids and basement nature of the Junggar Terrane, NW China: Nd–Sr isotope and trace element evidence. Journal Asian Earth Sciences 23, 691–703.
Chen, B., Jahn, B.M., 2002. Geochemical and isotopic studies of the sedimentary and granitic rocks of the Altai orogen of NW China and their tectonic implications. Geological Magazine 39, 1–13.
Chen, B., Arakawa, Y., 2005. Elemental and Nd–Sr isotopic geochemistry of granitoids from the West Junggar foldbelt (NW China), with implications for Phanerozoic continental growth. Geochimica et Cosmochimica Acta 69, 1307–1320.
Clague, D.A., Frey, F.A., 1982. Petrology and trace element geochemistry of the Honolulu Volcanics, Oahu: implications for the oceanic mantle below Hawaii. Journal of Petrology 23, 447–504.
Cocks, L.R.M., Torsvik, T.H., 2007. Siberia, the wandering northern terrane, and its changing geography through the Palaeozoic. Earth-Science Reviews 82, 29–74.

Please cite this article as: Zhang, Z., et al., Late Paleozoic volcanic record of the Eastern Junggar terrane, Xinjiang, Northwestern China: Major and trace element characteristics, Sr–Nd isotopic systematics and implications ..., Gondwana Research (2009), doi:10.1016/j.gr.2009.03.004

Coleman, R.G., 1989. Continental growth of northwestern China. Tectonics 8, 621–635.
Davidson, J.P., 1996. Deciphering mantle and crustal signatures in subduction zone magmatism. Subduction Top to Bottom. Geophys., Monogr, vol. 96. American Geophysical Union, Washington D C, pp. 251–262.
Defant, M.J., Drummond, M.S., 1990. Derivation of some modern arc magmas by melting of young subducted lithosphere. Nature 347, 662–665.
de Jong, K., Xiao, W.J., Windley, B.F., Masago, H., Lo, C.H., 2006. Ordovician $^{40}Ar/^{39}Ar$ phengite ages from the blueschist-facies Ondor Sum subduction–accretion complex (Inner Mongolia) and implications for the early Paleozoic history of continental blocks in China and adjacent areas. American Journal of Science 306, 799–845.
de Jong, K., Wang, B., Faure, M., Shu, L.S., Cluzel, D., Charvet, J., Ruffet, G., Chen, Y., 2008. New 40Ar/39Ar age constraints on the Late Palaeozoic tectonic evolution of the western Tianshan (Xinjiang, northwestern China), with emphasis on late Permian fluid ingress. International Journal of Earth Sciences. doi:10.1007/s00531-008-0338-8.
Deng, J.H., Wang, D.Y., 1995. Characteristics and tectonic significance of ophiolite zones in Zaheba region, Fuyun county, Xinjiang. Journal of Chengdu University Technology 22, 8–14 (in Chinese with English abstract).
Drummond, M.S., Defant, M.J., 1990. A model for trondhjemite–tonalite–dacite genesis and crustal growth via slab melting: Archean to modern comparisons. Journal of Geophysical Research 95, 21503–21521.
Dulski, P., 1994. Interferences of oxide, hydroxide and chloride analyses species in the determination of rare earth elements in geological samples by inductively coupled plasma-mass spectrometry. Fresenius's Journal of Analytical Chemistry 350, 194–203.
Ellam, R.M., Cox, K.G., 1989. A Proterozoic lithospheric source for Karoo magmatism: evidence from the Nuanetsi picrites. Earth and Planetary Science Letters 92, 207–218.
Fedorenko, V.A., Doherty, W., 1993. Remobilisation of the continental lithosphere by a mantle plume: major-, trace element and Sr-, Nd-, and Pb-isotope evidence from picritic and tholeiitic lavas of the Noril'sk District, Siberian Trap, Russia. Contributions to Mineralogy and Petrology 114, 171–188.
Feng, Y., Coleman, R.G., Tilton, G., Xiao, X., 1989. Tectonic evolution of the West Junggar region, Xinjiang, China. Tectonics 8, 729–752.
Filippova, I.B., Bush, V.A., Didenko, A.N., 2001. Middle Paleozoic subduction belts: the leading factor in the formation of the Central Asian fold-and-thrust belt. Russian Journal of Earth Sciences 3, 405–426.
Fleming, T.H., Elliot, D.H., Jones, L.M., Bowman, J.R., Siders, M.A., 1992. Chemical and isotopic variations in an iron-rich lava flow from the Kirkpatrick Basalt, North Victoria Land, Antarctica: implications for low-temperature alteration. Contributions to Mineralogy and Petrology 111, 440–457.
Goldfarb, R.J., Mao, J.W., Hart, C., Wang, D.H., Anderson, E., Wang, Z.L., 2003. Tectonic and metallogenic evolution of the Altay Shan, Northern Xinjiang Uygur Autonomous Region, Northwestern China. In: Mao, J., Goldfarb, R.J., Seltmann, R. (Eds.), Tectonic Evolution and Metallogeny of the Chinese Altay and Tianshan. IAGOD Guidebook Series, vol. 10, pp. 17–30. London.
Gradstein, F.M., Ogg, J.G., Smith, A.G. (Eds.), 2004. A Geologic Time Scale 2004. Cambridge University Press, Cambridge. 610 pp.
Han, B.F., 1991. The middle Devonian bimodal association of volcanic rocks in the northern area of east Junggar, Xinjiang. Acta Geologica Sinica 65, 317–326 (in Chinese with English abstract).
Han, B., Ji, J., Song, B., Chen, L., Li, Z., 2004. SHRIMP zircon U–Pb ages of Kalatongke No. 1 and Huangshandong Cu–Ni-bearing mafic–ultramafic complexes, North Xinjiang, and geological implications. Chinese Science Bulletin 49, 2424–2429.
Harmer, R.H., Eglington, B.M., Farrow, D., Butcher, A.R., Auret, J.M., Stander, Y.Y., Grosser, E., 1986. Manual of laboratory procedures for isotope analysis. Int Rep. National Physical Research Laboratory. CSIR, Pretoria.
Hawkesworth, C.J., Marsh, J.S., Duncan, A.R., Erlank, A.J., Norry, M.J., 1984. The role of continental lithosphere in the generation of the Karoo volcanic rocks: evidence from combined Nd- and Sr-isotope studies. In: Erlank, A.J. (Ed.), Petrogenesis of the Volcanic Rocks of the Karoo Province. Geological Society of South Africa, Special. Publication, vol. 13, pp. 341–354.
He, G., Li, M.S., Liu, D.Q., Tang, Y.L., Zhou, R.H., 1994. Paleozoic Crustal Evolution and Mineralization in Xinjiang of China. Xinjiang People's Publishing House, Urumchi. (in Chinese).
Hergt, J., Peate, D., Hawkesworth, C.J., 1991. The petrogenesis of Mesozoic Gondwana low-Ti flood basalts. Earth and Planetary Science Letters 105, 134–148.
Heubeck, C., 2001. Assembly of Central Asia during the middle and late Paleozoic. In: Hendrix, M.S., Davis, G.A. (Eds.), Paleozoic and Mesozoic Tectonic Evolution of Central and Eastern Asia. Geological Society of American memoirs, vol. 194, pp. 1–22.
Hochstaedter, A.G., Gill, J.B., Kusakabe, M., 1990a. Volcanism in the Sumisu Rift. I. Element, volatile and stable isotope geochemistry. Earth and Planetary Science Letters 100, 179–194.
Hochstaedter, A.G., Gill, J.B., Morris, J., 1990b. Volcanism in the Sumisu Rift. II. Subduction and nonsubduction related components. Earth and Planetary Science Letters 100, 195–209.
Hollings, P., Kerrich, R., 2004. Geochemical systematics of tholeiites from the 2.86 Ga Pickle Crow Assemblage, northwestern Ontario: arc basalts with positive and negative Nb–Hf anomalies. Precambrian Research 134, 1–20.
Hong, D.W., Wang, S.G., Xie, X.L., Zhang, J.S., Wang, T., 2003a. Metallogenic province derived from mantle sources: Nd, Sr, S and Pb isotope evidence from the Central Asian Orogenic Belt. Gondwana Research 6, 711–728.
Hong, D.W., Wang, S.G., Xie, X.L., Zhang, J.S., Wang, T., 2003b. Grantoids and related metallogeny of the Central Asian Orogenic Belt. In: Mao, J., Goldfarb, R.J., Seltmann, R. (Eds.), Tectonic Evolution and Metallogeny of the Chinese Altay and Tianshan. IAGOD Guidebook Series, vol. 10, pp. 75–106. London.
Jahn, B.M., Wu, F., Chen, B., 2000. Granitoids of the Central Asian Orogenic Belt and continental growth in the Phanerozoic. Transactions of the Royal Society of Edinburgh: Earth Sciences 91, 181–193.
Jahn, B.M., 2004. The Central Asian Orogenic Belt evolution and growth of the continental crust in the Phanerozoic. In: Malpas, J., Fletcher, C.J.N., Ali, J.R., Aichison, J.C. (Eds.), Aspects of the Tectonic Evolution of China. Geological Society, London, Special Publications, vol. 226, pp. 73–100.
Jian, P., Liu, D.Y., Zhang, Q., Zhang, F.Q., Shi, Y.R., Shi, G.H., Zhang, L.Q., Tao, H., 2003. SHRIMP dating of ophiolite and leucocratic rocks within ophiolite. Earth Science Frontiers 10, 439–455 (in Chinese with English abstract).
Khain, E.V., Bibikova, E.V., Salnikova, E.B., Kröner, A., Gibsher, A.S., Didenko, A.N., Degtyarev, K.E., Fedotova, A.A., 2003. The Palaeo-Asian ocean in the Neoproterozoic and early Paleozoic: new geochronologic data and palaeotectonic reconstructions. Precambrian Research 122, 329–358.
Kovalenko, V.I., Yarmolyuk, V.V., Kovach, V.P., Kotov, A.B., Kozakov, I.K., Salnikova, E., Larin, A.M., 2004. Isotope provinces, mechanisms of generation and sources of the continental crust in the Central Asian mobile belt: geological and isotopic evidence. Journal of Asian Earth Sciences 23, 605–627.
Kröner, A., Windley, B.F., Badarch, G., Tomurtogoo, O., Hegner, E., Liu, D.Y., Wingate, M.T.D., 2007. Accretionary growth and crust formation in the Central Asian Orogenic Belt and comparison with the Arabian–Nubian shield. In: HatcherJr. Jr., R.D., Carlson, M.P., McBride, J.H., Martínez Catalán, J.R. (Eds.), 4-D Framework of Continental Crust. Geological Society of America Memoir, vol. 200, pp. 181–209.
Kuzmichev, A., Kröner, A., Hegner, E., Liu, D., Wan, Y., 2005. The Shishkhid ophiolite, northern Mongolia: a key to the reconstruction of a Neoproterozoic island-arc system in central Asia. Precambrian Research 138, 125–150.
Lamb, M.A., Badarch, G., 2000. Paleozoic sedimentary Basin and volcanic arc systems if southern Mongolia: new stratigraphic and sedimentologic constraints. In: Ernst, W.G., Coleman, R.G. (Eds.), Tectonic Studies of Asia and the Pacific Rim. Bellwether Publishing Ltd for the Geological Society of America, pp. 107–141.
Le Maitre, R.W. (Ed.), 1989. A Classification of Igneous Rocks and Glossary of Terms. Wiley. 236 pp.
Li, J., Xiao, W., Wang, K., Sun, G., Gao, A., 2003. Neoproterozoic to Paleozoic tectonostratigraphy, magmatic activities and tectonic evolution of eastern Xinjiang, NW China. In: Mao, J., Goldfarb, R.J., Seltmann, R. (Eds.), Tectonic Evolution and Metallogeny of the Chinese Altay and Tianshan. IAGOD Guidebook Series, vol. 10, pp. 31–74. London.
Lindstrom, M.M., Haskin, L.A., 1981. Compositional heterogeneities in a single Icelandic tholeiite flow. Geochimica et Cosmochimica. Acta 45, 15–31.
Liu, J., Li, Y.J., Wang, X.G., Guo, W.J., 2006. Geochemical characteristics and tectonic environment of the Yishijilike Formation volcanic rocks in the Awulale area of western Tianshan. Xinjiang Geology 24, 105–108 (in Chinese with English abstract).
Long, X.P., Sun, M., Yuan, C., Xiao, W.J., Chen, H.L., Zhao, Y.J., Cai, K.D., Li, J.L., 2005. Genesis of Carboniferous volcanic rocks in the eastern Junggar: constraints on the closure of the Junggar Ocean. Acta Petrologica Sinica 22, 31–40 (in Chinese with English abstract).
Mahoney, J.J., 1988. Deccan Traps. In: Macdougall, J.D. (Ed.), Continental Flood Basalts. Kluwer Academic Publishers, Dordrecht, pp. 151–194.
Mao, J.W., Pirajno, F., Zhang, Z.H., Chai, F.M., Wu, H., Chen, S.P., Cheng, S.L., Yang, J.M., Zhang, C., 2008. Late Hercynian post-collisional Cu–Ni sulphide deposits in the Chinese Tianshan and Altay orogens (Xinjiang Province): principal characteristics and ore-forming processes. Journal of Asian Earth Science 32, 184–203.
Martin, H., 1999. Adakitic magmas: modern analogues of Archean granitoids. Lithos 46, 411–429.
Mei, H.J., Yang, X.C., Wang, J.D., Yu, X.Y., Liu, T.G., Bai, Z.H., 1993. Trace element geochemistry of late Paleozoic volcanic rocks on the southern side of the Irtysh River and the evolutionary history of tectonic setting. In: Tu, G.Z. (Ed.), Progress of Solid-Earth Sciences in Northern Xinjiang, China. Science Press, Beijing, pp. 199–216 (in Chinese).
Meschede, M., 1986. A model of discriminating between different type of mid-ocean ridge and continental tholeiites with the Nb–Zr–Y diagram. Chemical Geology 56, 207–218.
Miyashiro, A., 1975. Classification, characteristics and origin of ophiolites. The Journal of Geology 83, 249–281.
Mossakovsky, A.A., Ruzhentsev, S.V., Samygin, S.G., Kheraskova, T.N., 1994. Central Asian foldbelt: geodynamic evolution and formation history. Geotectonics 27, 445–474.
Norrish, K., Chappel, B.W., 1977. X-ray fluorescence spectrometry, In: Zussman, J. (Ed.), Physical Methods in Determinative Mineralogy, 2nd edn. Academic Press, New York, pp. 201–272.
Pearce, J.A., Norry, M.J., 1979. Petrogenetic implications of Ti, Zr, Y and Nb variations in volcanic rocks. Contributions to Mineralogy and Petrology 69, 33–47.
Peng, Z.Z., Mahoney, J.J., 1995. Drill-hole lavas from the northwestern Deccan Traps, and the evolution of Reúnion hotspot mantle. Earth and Planetary Science Letters 134, 169–185.
Ping, J., Dunyi, L., Yuruo, S., Fuqin, Z., 2005. SHRIMP dating of SSZ ophiolites from northern Xinjiang Province, China: implications for generation of oceanic crust in the Central Asian Orogenic Belt. In: Sklyarov, E.V. (Ed.), Structural and Tectonic Correlation across the Central Asia Orogenic Collage: North-Eastern Segment. Guidebook and Abstract Volume of the Siberian Workshop IGCP-480. IEC SB RAS, Irkutsk, p. 246.
Pirajno, F., Mao, J., Zhang, Z.C., Zhang, Z.H., Chai, F.M., 2008. The association of mafic–ultramafic intrusions and A-type magmatism in the Tian Shan and Altay orogens, NW China: implications for geodynamic evolution and potential for the discovery of new ore deposits. Journal of Asian Earth Sciences 32, 165–183.
Schiano, P., Clocchiatti, R., Shimizu, N., Maury, R.C., Jochum, K.P., Hofmann, A.W., 1995. Hydrous, silica-rich melts in the sub-arc mantle and their relationship with erupted arc lavas. Nature 377, 595–600.
Safonova, I.Y., Buslov, M.M., Iwata, K., Kokh, D.A., 2002. Fragments of Vendian–Early Carboniferous oceanic crust of the Paleo-Asian Ocean in foldbelts of the Altai–Sayan region of Central Asia: geochemistry, biostratigraphy and structural setting. Gondwana Research 7, 771–790.

Sengör, A.M.C., Natal'in, B.A., 1996. Turkic-type orogeny and its role in the making of the continental crust. Annual Review Earth and Planetary Science Letters 24, 263–337.
Sengör, A.M.C., Natal'in, B.A., 2004. Phanerozoic analogs of Archean oceanic basement fragments: altaid ophiolites and ophiorags. In: Kusky, T.M. (Ed.), Precambrian Ophiolites and Related Rocks. Developments in Precambrian Geology, vol. 13. Elsevier, Amsterdam, pp. 675–726.
Sengör, A.M.C., Natal'in, B.A., Burtman, V.S., 1993. Evolution of the Altaid tectonic collage and Paleozoic crustal growth in Eurasia. Nature 364, 299–307.
Sun, S.S., McDonough, W.F., 1989. Chemical and isotopic systematics of oceanic basalts: implications for mantle composition and processes. In: Saunders, A.D., Norry, M.J. (Eds.), Magmatism in the Ocean Basins. Special Publication, vol. 42. Geological Society, London, pp. 313–345.
Sun, L.H., Wang, Y.J., Fan, W.M., Zi, J.W., 2008. Post-collisional potassic magmatism in the Southern Awulale Mountain, western Tianshan Orogen: petrogenetic and tectonic implications. Gondwana Research 14, 383–394.
Tang, H.F., Su, Y.P., Liu, C.Q., Hou, G.S., Wang, Y.B., 2007. Zircon U–Pb age of the Plagiogranite in Kalamali belt, Northern Xinjiang and its tectonic implications. Geotectonica et Metallogenia 31, 110–117 (in Chinese with English abstract).
Wang, D.H., Chen, Y.C., Xu, Z.G., Li, T.D., Fu, X.J., 2002. Metallogenic Series and Regularities in Altay Metallogenic Province. Atomic Energy Press, Beijing. 493 pp. (in Chinese).
Wang, B., Cluzel, D., Shu, L.S., Faure, M., Chen, Y., Meffre, S., Charvet, J., de Jong, K., 2009. Evolution of calc-alkaline to alkaline magmatism through Carboniferous convergence to Permian transcurrent tectonics, western Chinese Tianshan. International Journal of Earth Sciences. doi:10.1007/s00531-008-0408-y.
Wei, G.Y., Ni, Z.Y., 1990. Preliminary study of the rift volcanic rocks of the Irtysh volcanic area, Xinjiang. Journal of Mineralogy and Petrology 10, 15–23 (in Chinese with English abstract).
Winchester, J.A., Floyd, P.A., 1977. Geological discrimination of different magma series and their differentiation products using immobile elements. Chemical Geology 20, 325–343.
Windley, B.F., Allen, M.B., Zhang, C., Zhao, Z.Y., Wang, G.R., 1990. Paleozoic accretion and Cenozoic redeformation of the Chinese Tien Shan Range, Central Asia. Geology 18, 128–131.
Windley, B.F., Kröner, A., Guo, J.H., Qu, G.S., Li, Y.Y., Zhang, C., 2002. Neoproterozoic to Paleozoic geology of the Altai orogen, NW China: new zircon age data and tectonic evolution. The Journal of Geology 110, 719–737.
Wooden, J.L., Czamanske, G.K., Fedorenko, V.A., Arndt, N.T., Chauvel, C., Bouse, R.M., King, B.S.W., Knight, R.J., Siems, D.F., 1993. Isotopic and trace-element constraints on mantle and crustal contributions to Siberian continental flood basalts, Noril'sk area, Siberia. Geochimica et Cosmochimica Acta 57, 3704–3766.
Wu, F.Y., Jahn, B.M., Wilde, S., Sun, D.Y., 2000. Phanerozoic crustal growth: U–Pb and Sr–Nd isotopic evidence from the granites in northeastern China. Tectonophysics 328, 89–113.
Xia, L.Q., Xu, X.Y., Xia, Z.C., Li, X.M., Ma, Z.P., Wang, L.S., 2004. Petrogenesis of Carboniferous rift-related volcanic rocks in the Tianshan, northwestern China. Geological Society of American Bulletin 116, 419–433.
Xiao, W.J., Windley, B.F., Hao, J., Zhai, M.G., 2003. Accretion leading to collision and the Permian Solonker suture, Inner Mongolia, China: termination of the Central Asian Orogenic Belt. Tectonics 22, 1–20.
Xiao, W.J., Windley, B.F., Badararch, G., Sun, S., Li, J., Qin, K., Wang, Z., 2004. Paleozoic accretionary and convergent tectonics of the southern Altaids: implications for the growth of central Asia. Journal of the Geological Society, London 161, 339–342.
Xiao, W.J., Han, C.M., Yuan, C., Sun, M., Lin, S.F., Chen, H.L., Li, Z.L., Li, J.L., Sun, S., 2008. Middle Cambrian to Permian subduction-related accretionary orogenesis of Northern Xinjiang, NW China: implications for the tectonic evolution of central Asia. Journal of Asian Earth Sciences 32, 102–117.
Xu, J.F., Mei, H.J., Yu, X.Y., 2001. Adakites related to subduction in the northern margin of Junggar arc for the Late Paleozoic: products of slab melting. Chinese Science Bulletin 46, 684–688.
Xu, X.Y., Ma, Z.P., Xia, Z.C., Xia, L.Q., Li, X.M., Wang, L.S., 2006. TIMS U–Pb isotopic dating and geochemical characteristics of Paleozoic granitic rocks from the Middle-Western section of Tianshan. Northwestern Geology 39, 50–75 (in Chinese with English abstract).
Yan, S.H., Chen, W., Wang, Y.T., Zhang, Z.C., Chen, B.L., 2005. Rare earth element geochemistry of the Qiaoxiahala Fe–Cu deposit in the south margin of the Altay Mts. and its implication. Mineral Deposita 24, 25–33 (in Chinese with English abstract).
Yang, F.Q., Wu, H., Zhang, Y.L., Fu, X.J., 2001. Volcanic rocks and geochemical characteristics of the Batamayineishan Formation in Jinshangou, Xinjiang. Journal of Xi'an Engineer University 23, 20–25 (in Chinese with English abstract).
Yu, X.Y., Mei, H.J., Yang, X.C., 1993. Volcanic rocks and tectonic evolution of the Irtysh region. In: Guangchi, Tu (Ed.), New Progress of Solid Earth Sciences of the Northern Xinjiang. Science Press, Beijing, pp. 185–198 (in Chinese).
Zhai, M.G., Xiao, W.J., Kusky, T., Santosh, M., 2007. Tectonic evolution of China and adjacent crustal fragments. Gondwana Research 12, 1–3.
Zhang, H.X., Niu, H.C., Hiroaki, S., Shan, Q., Yu, X.Y., Jun ' ichi, I., Zhang, Q., 2004. Late Paleozoic adakite and Nb-enriched basalt from northern Xinjiang: evidence for the southward subduction of the Paleo-Asian Ocean. Geological Journal of China Universities 10, 106–113 (in Chinese with English abstract).
Zhang, Z.C., Yan, S.H., Chen, B.L., Zhou, G., He, Y.K., Chai, F.M., He, L.X., Wan, Y.S., 2006. SHRIMP zircon U–Pb dating for subduction-related granitic rocks in the northern part of east Junggar, Xinjiang. Chinese Science Bulletin 51, 952–962.
Zhang, Z.H., Mao, J.W., Du, A.D., Pirajno, F., Wang, Z.L., Chai, F.M., Zhang, Z.C., Yang, J.M., 2008a. Re–Os dating of two Cu–Ni sulfide deposits in northern Xinjiang and its geological significance. Journal of Asian Earth Sciences 32, 204–217.
Zhang, Z.C., Mao, J.W., Cai, J.H., Zhou, G., Yan, S.H., Kusky, T.M., 2008b. Geochemistry of picrites and associated lavas of a Devonian island arc in the Northern Junggar terrane, Xinjiang (NW China): implications for petrogenesis, arc mantle sources and tectonic setting. Lithos 105, 379–395.
Zhang, Z.C., Kusky, T.M., Mao, J.W., Zhao, L., Yan, S.H., Chen, B.L., Zhou, G., Chai, F.M., 2008c. Geochronology and geochemistry of the Kuwei mafic intrusion, southern margin of the Altai Mountains, Northern Xinjiang, NW China: evidence for distant effects of the Indo-Eurasia collision. The Journal of Geology 116, 119–133.
Zhao, Z., Xiong, X., Wang, Q., Bai, Z., Qiao, Y., 2009-this issue. Late Paleozoic underplating in North Xinjiang. Gondwana Research.
Zheng, J.P., Sun, M., Zhao, G.C., Robinson, P.T., Wang, F.Z., 2007. Elemental and Sr–Nd–Pb isotopic geochemistry of Late Paleozoic volcanic rocks beneath the Junggar basin, NW China: implications for the formation and evolution of the basin basement. Journal of Asian Earth Sciences 29, 778–794.
Zhu, Z.X., Li, S.Z., Li, G.L., 2005. The characteristics of sedimentary system —continental facies volcano in later Carboniferous Batamayi group, Zhifang region, East Junggar. Xinjiang Geology 23, 14–18 (in Chinese with English abstract).

Please cite this article as: Zhang, Z., et al., Late Paleozoic volcanic record of the Eastern Junggar terrane, Xinjiang, Northwestern China: Major and trace element characteristics, Sr–Nd isotopic systematics and implications ..., Gondwana Research (2009), doi:10.1016/j.gr.2009.03.004